

University of Texas Rio Grande Valley

ScholarWorks @ UTRGV

Physics and Astronomy Faculty Publications
and Presentations

College of Sciences

11-18-2016

Results of the deepest all-sky survey for continuous gravitational waves on LIGO S6 data running on the Einstein@Home volunteer distributed computing project

B. P. Abbott

R. Abbott

T. D. Abbott

M. R. Abernathy

F. Acernese

See next page for additional authors

Follow this and additional works at: https://scholarworks.utrgv.edu/pa_fac



Part of the [Astrophysics and Astronomy Commons](#)

Recommended Citation

B. P. Abbott, et. al., (2016) Results of the deepest all-sky survey for continuous gravitational waves on LIGO S6 data running on the Einstein@Home volunteer distributed computing project. *Physical Review D* 94:10. DOI: <http://doi.org/10.1103/PhysRevD.94.102002>

This Article is brought to you for free and open access by the College of Sciences at ScholarWorks @ UTRGV. It has been accepted for inclusion in Physics and Astronomy Faculty Publications and Presentations by an authorized administrator of ScholarWorks @ UTRGV. For more information, please contact justin.white@utrgv.edu, william.flores01@utrgv.edu.

Authors

B. P. Abbott, R. Abbott, T. D. Abbott, M. R. Abernathy, F. Acernese, K. Ackley, C. Adams, T. Adams, P. Addesso, R. X. Adhikari, V. B. Adya, C. Affeldt, M. Agathos, K. Agatsuma, N. Aggarwal, O. D. Aguiar, L. Aiello, A. Ain, B. Allen, A. Allocca, P. A. Altin, S. B. Anderson, W. G. Anderson, K. Arai, M. C. Araya, C. C. Arceneaux, J. S. Areeda, N. Arnaud, K. G. Arun, and S. Ascenzi

Results of the deepest all-sky survey for continuous gravitational waves on LIGO S6 data running on the Einstein@Home volunteer distributed computing project

B. P. Abbott *et al.**(LIGO Scientific Collaboration and Virgo Collaboration)
(Received 6 July 2016; published 18 November 2016)

We report results of a deep all-sky search for periodic gravitational waves from isolated neutron stars in data from the S6 LIGO science run. The search was possible thanks to the computing power provided by the volunteers of the Einstein@Home distributed computing project. We find no significant signal candidate and set the most stringent upper limits to date on the amplitude of gravitational wave signals from the target population. At the frequency of best strain sensitivity, between 170.5 and 171 Hz we set a 90% confidence upper limit of 5.5×10^{-25} , while at the high end of our frequency range, around 505 Hz, we achieve upper limits $\approx 10^{-24}$. At 230 Hz we can exclude sources with ellipticities greater than 10^{-6} within 100 pc of Earth with fiducial value of the principal moment of inertia of 10^{38} kg m². If we assume a higher (lower) gravitational wave spin-down we constrain farther (closer) objects to higher (lower) ellipticities.

DOI: [10.1103/PhysRevD.94.102002](https://doi.org/10.1103/PhysRevD.94.102002)

I. INTRODUCTION

In this paper we report the results of a deep all-sky Einstein@Home [1] search for continuous, nearly monochromatic gravitational waves (GWs) in data from LIGO's sixth science (S6) run. A number of all-sky searches have been carried out on LIGO data, [2–11], of which [5,7,10] also ran on Einstein@Home. The search presented here covers frequencies from 50 Hz through 510 Hz and frequency derivatives from 3.39×10^{-10} Hz/s through -2.67×10^{-9} Hz/s. In this range we establish the most constraining gravitational wave amplitude upper limits to date for the target signal population.

II. LIGO INTERFEROMETERS AND THE DATA USED

The LIGO gravitational wave network consists of two observatories, one in Hanford (WA) and the other in Livingston (LA) separated by a 3000-km baseline [12]. The last science run (S6) [13] of this network before the upgrade towards the advanced LIGO configuration [14] took place between July 2009 and October 2010. The analysis in this paper uses a subset of this data: from GPS 949469977 (2010 Feb 6 05:39:22 UTC) through GPS 971529850 (2010 Oct 19 13:23:55 UTC), selected for good strain sensitivity [15]. Since interferometers sporadically fall out of operation (“lose lock”) due to environmental or

instrumental disturbances or for scheduled maintenance periods, the data set is not contiguous and each detector has a duty factor of about 50% [16].

As done in [7], frequency bands known to contain spectral disturbances have been removed from the analysis. Actually, the data has been substituted with Gaussian noise with the same average power as that in the neighboring and undisturbed bands. Table III identifies these bands.

III. THE SEARCH

The search described in this paper targets nearly monochromatic gravitational wave signals as described for example by Eqs. 1–4 of [7]. Various emission mechanisms could generate such a signal as reviewed in Sec. II A of [11]. In interpreting our results we will consider a spinning compact object with a fixed, nonaxisymmetric mass quadrupole, described by an ellipticity ϵ .

We perform a stack-slide type of search using the GCT (Global Correlation Transform) method [17,18]. In a stack-slide search the data is partitioned in segments and each segment is searched with a matched-filter method [19]. The results from these coherent searches are combined by summing (stacking) the detection statistic values from the segments (sliding), one per segment (\mathcal{F}_i), and this determines the value of the core detection statistic:

$$\overline{\mathcal{F}} := \frac{1}{N_{\text{seg}}} \sum_{i=1}^{N_{\text{seg}}} \mathcal{F}_i. \quad (1)$$

There are different ways to combine the single-segment \mathcal{F}_i values, but independently of the way that this is done, this type of search is usually referred to as a “semicoherent

*Full author list given at end of the article.

Published by the American Physical Society under the terms of the *Creative Commons Attribution 3.0 License*. Further distribution of this work must maintain attribution to the author(s) and the published article's title, journal citation, and DOI.

search”. So stack-slide searches are a type of semicoherent search. Important variables for this type of search are the coherent time baseline of the segments T_{coh} , the number of segments used N_{seg} , the total time spanned by the data T_{obs} , the grids in parameter space and the detection statistic used to rank the parameter space cells. For a stack-slide search in Gaussian noise, $N_{\text{seg}} \times 2\overline{\mathcal{F}}$ follows a $\chi^2_{4N_{\text{seg}}}$ chi-squared distribution with $4N_{\text{seg}}$ degrees of freedom. These parameters are summarized in Table I. The grids in frequency and spin-down are each described by a single parameter, the grid spacing, which is constant over the search range. The same frequency grid spacings are used for the coherent searches over the segments and for the incoherent summing. The spin-down spacing for the incoherent summing, $\delta\dot{f}$, is finer than that used for the coherent searches, $\delta\dot{f}_c$, by a factor γ . The notation used here is consistent with that used in previous observational papers [20] and in the GCT methods papers cited above.

The sky grid is the union of two grids: one is uniform over the projection of the celestial sphere onto the equatorial plane, and the tiling (in the equatorial plane) is approximately square with sides of length

$$d(m_{\text{sky}}) = \frac{1}{f} \frac{\sqrt{m_{\text{sky}}}}{\pi\tau_E}, \quad (2)$$

with $m_{\text{sky}} = 0.3$ and $\tau_E \approx 0.021$ s being half of the light travel time across the Earth. As was done in [7], the sky-grids are constant over 10 Hz bands and the spacings are the ones associated through Eq. (2) to the highest frequency f in the range. The other grid is limited to the equatorial region ($0 \leq \alpha \leq 2\pi$ and $-0.5 \leq \delta \leq 0.5$), with constant right ascension α and declination δ spacings equal to $d(0.3)$ —see Fig. 1. The reason for the equatorial “patching” with a denser sky grid is to improve the sensitivity of the search: the sky resolution actually depends on the ecliptic latitude and the uniform equatorial grid under-resolves particularly in the equatorial region. The resulting number of templates used to search 50 mHz bands as a function of frequency is shown in Fig. 2.

The search is split into work-units (WUs) sized to keep the average Einstein@Home volunteer computer busy for about six hours. Each WU searches a 50 mHz band, the

TABLE I. Search parameters rounded to the first decimal figure. T_{ref} is the reference time that defines the frequency and frequency derivative values.

T_{coh}	60 hours
T_{ref}	960499913.5 GPS sec
N_{seg}	90
$\delta\dot{f}$	1.6×10^{-6} Hz
$\delta\dot{f}_c$	5.8×10^{-11} Hz/s
γ	230
m_{sky}	0.3 + equatorial patch

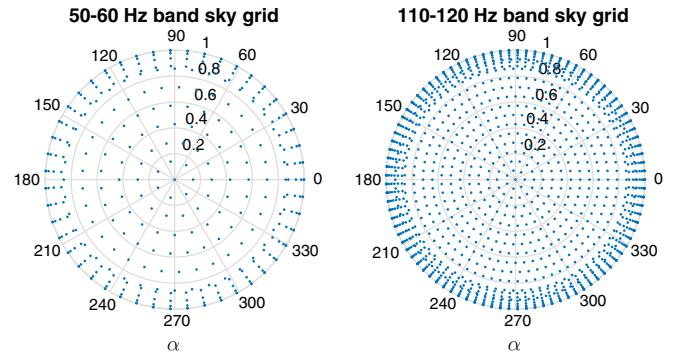


FIG. 1. Polar plots (r, θ plots with $\theta = \alpha$ and $r = \cos \delta$) of the grid points in the northern equatorial hemisphere sky for the band 50–60 Hz (left panel) and for the band 110–120 Hz (right panel). α is the right ascension coordinate and δ the declination coordinate. One can clearly see the higher density in the $-0.5 \leq \delta \leq 0.5$ equatorial region and the higher density ($\propto f^2$) of grid points at higher frequencies. The southern hemispheres looks practically identical to the respective northern ones.

entire spin-down range and 13 points in the sky, corresponding to 4.9×10^9 templates out of which it returns only the top 3000. A total of 12.7 million WUs are necessary to cover the entire parameter space. The total number of templates searched is 6.3×10^{16} .

A. The ranking statistic

The search was actually carried out in separate Einstein@Home runs that used different ranking statistics to define the top-candidate-list, reflecting different stages in the development of a detection statistic robust with respect

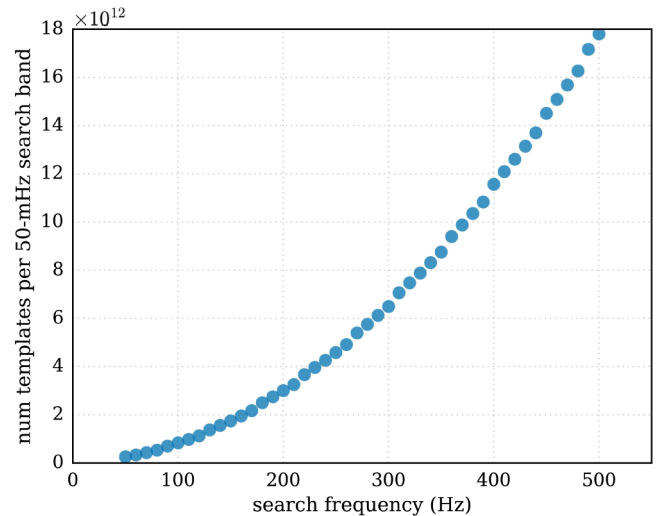


FIG. 2. Number of searched templates in 50 mHz bands. The variation with frequency is due to the increasing sky resolution. $N_f \times N_{\dot{f}} \sim 3.7 \times 10^8$, where N_f and $N_{\dot{f}}$ are the number of f and \dot{f} templates searched in 50 mHz bands. The total number of templates searched between 50 and 510 Hz is 6.3×10^{16} .

to spectral lines in the data [21]. In particular, three ranking statistics were used: the average $2\overline{\mathcal{F}}$ statistic over the segments, $2\overline{\mathcal{F}}$, which in essence at every template point is the likelihood of having a signal with the shape given by the template versus having Gaussian noise; the line-veto statistic \hat{O}_{SL} which is the odds ratio of having a signal versus having a spectral line; and a general line-robust statistic, \hat{O}_{SGL} , that tests the signal hypothesis against a Gaussian noise + spectral line noise model. Such a statistic can match the performance of both the standard average $2\overline{\mathcal{F}}$ statistic in Gaussian noise and the line-veto statistic in presence of single-detector spectral disturbances and statistically outperforms them when the noise is a mixture of both [21].

We combine the $2\overline{\mathcal{F}}$ -ranked results with the \hat{O}_{SL} -ranked results to produce a single list of candidates ranked according to the general line-robust statistic \hat{O}_{SGL} . We now explain how this is achieved. Alongside the detection statistic value and the parameter space cell coordinates of each candidate, the Einstein@Home application also returns the single-detector $2\overline{\mathcal{F}}^X$ values (“X” indicates the detector). These are used to compute, for every candidate of any run, the \hat{O}_{SGL} through Eq. 61 of [21]

$$\ln \hat{O}_{\text{SGL}} = \ln \hat{o}_{\text{SL}} + \hat{\mathcal{F}} - \hat{\mathcal{F}}''_{\text{max}} - \ln (e^{\hat{\mathcal{F}}_* - \hat{\mathcal{F}}''_{\text{max}}} + \langle \hat{\mathcal{F}}^X e^{\hat{\mathcal{F}}^X - \hat{\mathcal{F}}''_{\text{max}}} \rangle), \quad (3)$$

with the angle-brackets indicating the average with respect to detectors (X) and

$$\hat{\mathcal{F}} = N_{\text{seg}} \overline{\mathcal{F}} \quad (4)$$

$$\hat{\mathcal{F}}^X = N_{\text{seg}} \overline{\mathcal{F}}^X \quad (5)$$

$$\hat{\mathcal{F}}''_{\text{max}} \equiv \max(\hat{\mathcal{F}}_*, \hat{\mathcal{F}}^X + \ln \hat{\mathcal{F}}^X) \quad (6)$$

$$\hat{\mathcal{F}}_* \equiv \hat{\mathcal{F}}_*^{(0)} - \ln \hat{o}_{\text{LG}} \quad (7)$$

$$\hat{\mathcal{F}}_*^{(0)} \equiv \ln c_*^{N_{\text{seg}}} \quad \text{with } c_* \text{ set to } 20.64 \quad (8)$$

$$\hat{o}_{\text{LG}} = \sum_X \hat{o}_{\text{LG}}^X \quad (9)$$

$$\hat{\mathcal{F}}^X \equiv \frac{\hat{o}_{\text{LG}}^X}{\hat{o}_{\text{LG}}/N_{\text{det}}} \quad (10)$$

$$\hat{\rho}_{\text{L}} \equiv \frac{\hat{o}_{\text{LG}}}{1 + \hat{o}_{\text{LG}}}, \quad (11)$$

where \hat{o}_{LG}^X is the assumed prior probability of a spectral line occurring in any frequency bin of detector X, $\hat{\rho}_{\text{L}}$ is the line prior estimated from the data, $N_{\text{det}} = 2$ is the number of detectors, and \hat{o}_{SL} is an assumed prior probability of a line

being a signal (set arbitrarily to 1; its specific value does not affect the ranking statistic). Following the reasoning of Eq. 67 of [21], with $N_{\text{seg}} = 90$ we set $c_* = 20.64$ corresponding to a Gaussian false-alarm probability of 10^{-9} and an average $2\overline{\mathcal{F}}$ transition scale of ~ 6 ($\mathcal{F}_*^{(0)} \sim 3$). The \hat{o}_{LG}^X values are estimated from the data as described in Sec. VI. A of [21] in 50-mHz bands with a normalized-SFT-power threshold $\mathcal{P}_{\text{thr}}^X = \mathcal{P}_{\text{thr}}(p_{\text{FA}} = 10^{-9}, N_{\text{SFT}}^X \sim 6000) \approx 1.08$. For every 50 mHz band the list of candidates from the $2\overline{\mathcal{F}}$ -ranked run is merged with the list from the \hat{O}_{SL} -ranked run and duplicate candidates are considered only once. The resulting list is ranked by the newly computed \hat{O}_{SGL} and the top 3000 candidates are kept. This is our result-set, and it is treated in a manner that is very similar to [3].

B. Identification of undisturbed bands

Even after the removal of disturbed data caused by spectral artifacts of known origin, the statistical properties of the results are not uniform across the search band. In what follows we concentrate on the subset of the signal-frequency bands having reasonably uniform statistical properties. This still leaves us with the majority of the search parameter space while allowing us to use methods that rely on theoretical modeling of the significance in the statistical analysis of the results. Our classification of “clean” vs “disturbed” bands has no pretence of being strictly rigorous, because strict rigor here is neither useful nor practical. The classification serves the practical purpose of discarding from the analysis regions in parameter space with evident disturbances and must not dismiss real signals. The classification is carried out in two steps: a visual inspection and a refinement on the visual inspection.

The visual inspection is performed by three scientists who each look at various distributions of the detection statistics over the entire sky and spin-down parameter space in 50 mHz bands. They rank each band with an integer score 0,1,2,3 ranging from “undisturbed” (0) to “disturbed” (3). A band is considered “undisturbed” if all three rankings are 0. The criteria agreed upon for ranking are that the distribution of detection statistic values should not show a visible trend affecting a large portion of the $f - \dot{f}$ plane and, if outliers exist in a small region, outside this region the detection statistic values should be within the expected ranges. Figure 3 shows the \hat{O}_{SGL} for three bands: two were marked as undisturbed and the other as disturbed. One of the bands contains the $f - \dot{f}$ parameter space that harbors a fake signal injected in the data to verify the detection pipelines. The detection statistic is elevated in a small region around the signal parameters. The visual inspection procedure does not mark as disturbed bands with such features.

Based on this visual inspection 13% of the bands between 50 and 510 Hz are marked as “disturbed”. Of these, 34% were given by all visual inspectors rankings

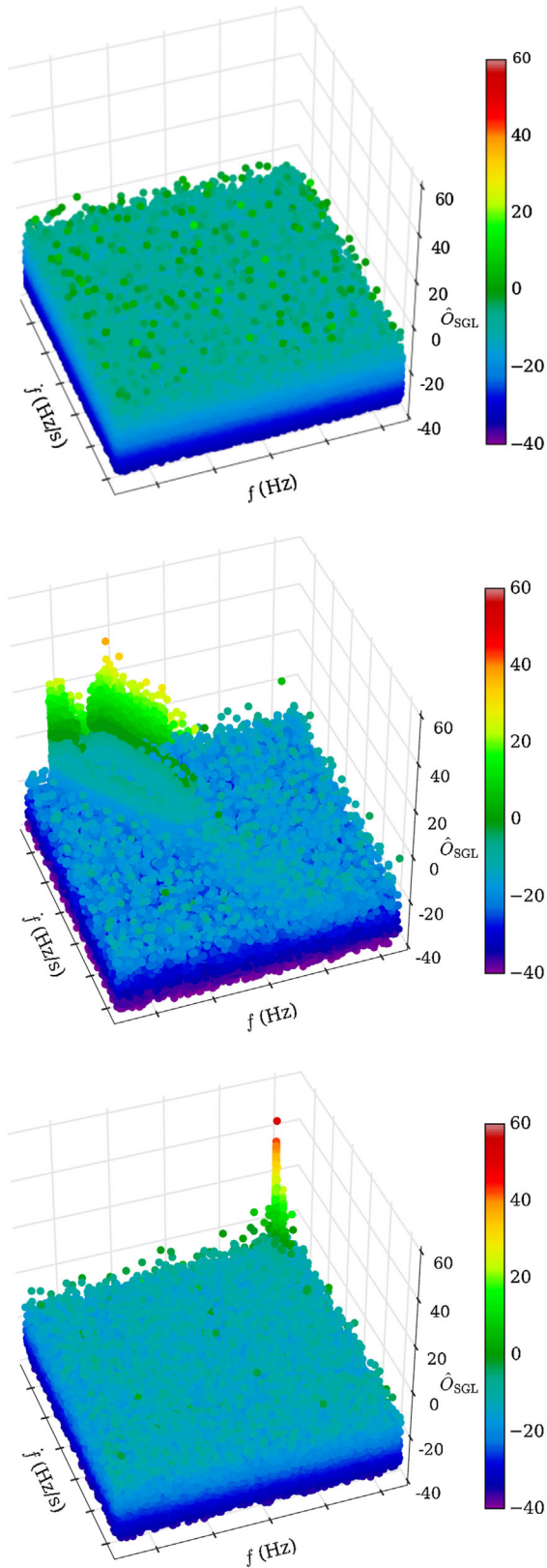


FIG. 3. On the z-axis and color-coded is the \hat{O}_{SGL} in three 50 mHz bands. The top band was marked as “undisturbed”. The middle band is an example of a “disturbed band”. The bottom band is an example of an “undisturbed band” but containing a signal, a fake one, in this case.

smaller than 3, i.e. they were only marginally disturbed. Further inspection “rehabilitated” 42% of these. As a result of this refinement in the selection procedure we exclude from the current analysis 11% of the searched frequencies (Table IV).

Figure 4 shows the highest values of the detection statistic in half-Hz signal-frequency bands compared to the expectations. The set of candidates that the highest detection statistic values are picked from, does not include the 50 mHz signal-frequency bands that stem entirely from fake data, from the cleaning procedure, or that were marked as disturbed. In this paper we refer to the candidates with the highest value of the detection statistic as the *loudest* candidates.

The loudest expected value over N_{trials} independent trials of $2\bar{\mathcal{F}}$ is determined¹ by numerical integration of the probability density function given, for example, by Eq. 7 of [20]. For this search, we estimate that $N_{\text{trials}} \approx 0.87N_{\text{templ}}$, with N_{templ} being the number of templates searched.

As a uniform measure of significance of the highest $2\bar{\mathcal{F}}$ value across bands that were searched with different values of N_{trials} we introduce the critical ratio CR defined as the deviation of the measured highest $2\bar{\mathcal{F}}$ from the expected value, measured in units of the standard deviation

$$\text{CR} := \frac{2\bar{\mathcal{F}}_{\text{meas}} - 2\bar{\mathcal{F}}_{\text{exped}}}{\sigma_{\text{exped}}}. \quad (12)$$

The highest and most significant detection statistic value from our search is $2\bar{\mathcal{F}} = 8.6$ at a frequency of about 52.76 Hz with a CR = 29. This is due to a fake signal. The second highest value of the detection statistic is 7.04 at a frequency of about 329.01 Hz corresponding to a CR of 4.6. The second highest-CR candidate has a $2\bar{\mathcal{F}}$ of 6.99, is

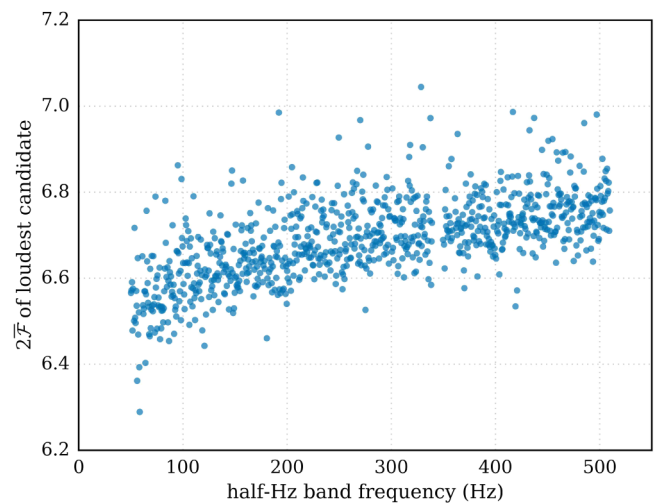


FIG. 4. Highest values of $2\bar{\mathcal{F}}$ in every half-Hz band as a function of band frequency. Since the number of templates increases with frequency so does the loudest $2\bar{\mathcal{F}}$.

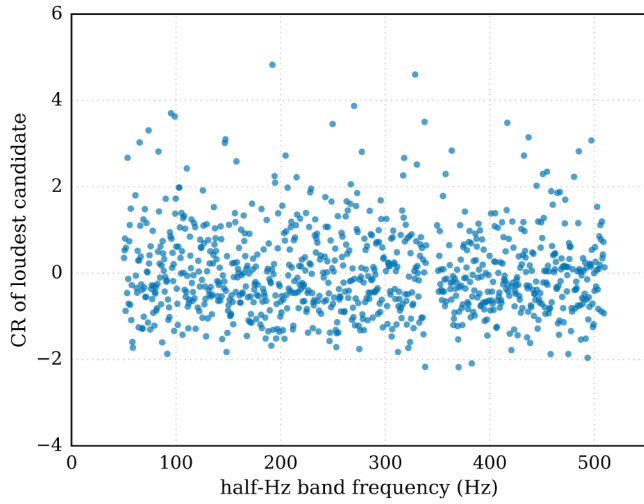


FIG. 5. Highest values of the significance (CR) in every half-Hz band as a function of band frequency. Since the significance folds in the expected value for the loudest $2\bar{\mathcal{F}}$ and its standard deviation, the significance of the loudest in noise does not increase with frequency. Our results are consistent with this expectation.

at 192.16 Hz and has a $CR = 4.8$. The CR values are plotted in Fig. 5, and the distribution in Fig. 6.

Sorting loudest candidates from half-Hz bands according to detection statistic values is not the same as sorting them according to CR. The reason for this is that the number of templates is not the same for all half-Hz bands. This is due to the grid spacings decreasing with frequency (Eq. (2)) and to the fact that, as previously explained, some 50 mHz bands have been excluded from the current analysis and hence some half-Hz bands comprise results from fewer than ten 50 mHz bands. Figure 7 gives the fill-level of each half-Hz band, i.e. how many 50 mHz bands have contributed candidates to the analysis out of ten. We use the CR as

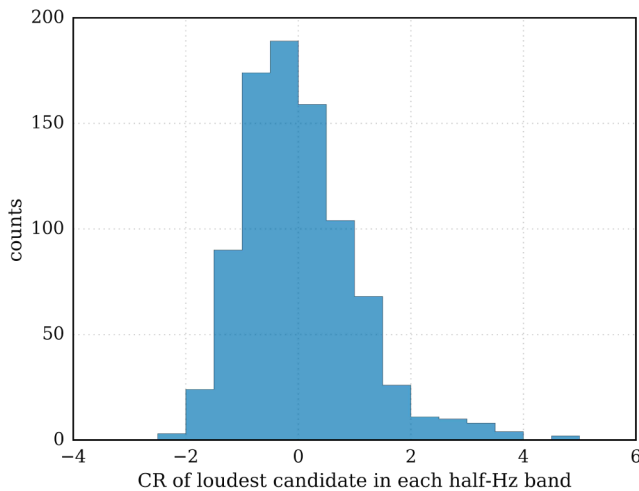


FIG. 6. Histogram of the highest values of the significance CR in every half-Hz band.

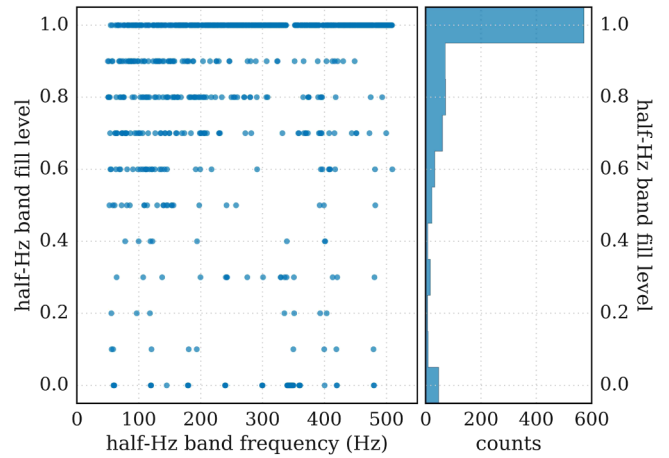


FIG. 7. The fraction of 50 mHz bands (in signal frequency) which contribute to the results in every half-Hz band. As explained in the text, some bands are excluded because they are all from fake data or because they are marked as disturbed by the visual inspection. The list of excluded bands is given in Table IV.

a measure of the significance because it folds in correctly the effect of varying number of templates in the half-Hz bands.

After excluding the candidate due to the fake signal, in this data we see no evidence of a signal: the distribution of p values associated with every measured half-Hz band loudest is consistent with what we expect from noise-only across the measured range (Fig. 8). In particular we note two things: 1) the two candidates at $CR = 4.6$ and $CR = 4.8$ are not significant when we consider how many half-Hz bands we have searched, and 2) there is no population of low significance candidates deviating from the expectation of the noise-only case. The p value for the loudest measured in any half-Hz band searched with an

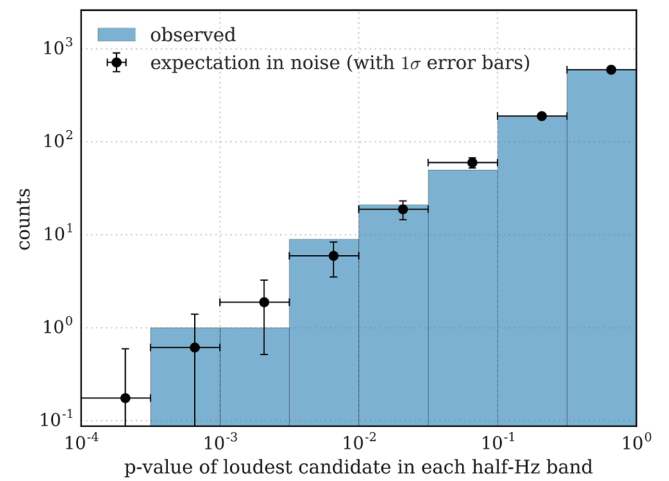


FIG. 8. p values for the loudest in half-Hz bands of our data (histogram bars) and expected distribution of pure noise data for reference (black markers).

effective number of independent trials $N_{\text{trials}} = 0.87N_{\text{trials}}$ is obtained by integrating Eq. 6 of [20] between the observed value and infinity.

IV. UPPER LIMITS

The search did not reveal any continuous gravitational wave signal in the parameter volume that was searched. We hence set frequentist upper limits on the maximum gravitational wave amplitude consistent with this null result in half-Hz bands: $h_0^{90\%}(f)$. $h_0^{90\%}(f)$ is the GW amplitude such that 90% of a population of signals with parameter values in our search range would have produced a candidate louder than what was observed by our search. This is the criterion hereafter referred to as “detection”.

Evaluating these upper limits with injection-and-recovery Monte Carlo simulations in every half-Hz band is too computationally intensive. So we perform them in a subset of 50 bands and infer the upper limit values in the other bands from these. The 50 bands are evenly spaced in the search frequency range. For each band $j = 1 \dots 50$, we measure the 90% upper limit value corresponding to different detection criteria. The different detection criteria are defined by different CR values for the assumed

measured loudest. The first CR bin, CR_0 , is for CR values equal to or smaller than 0, the next bins are for $i < \text{CR}_i \leq (i + 1)$ with $i = 1 \dots 5$. Correspondingly we have $h_{0, \text{CR}_i}^{90\%, j}$ for each band. For every detection criteria and every band we determine the sensitivity depth [22], and by averaging these sensitivity depths over the bands we derive a sensitivity depth for every detection criteria: $\mathcal{D}_{\text{CR}_i}^{90\%} = 1/50 \sum_j \mathcal{D}_{\text{CR}_i}^{90\%, j}$. We use these to set upper limits in the bands k where we have not performed injection-and-recovery simulations as

$$h_0^{90\%}(f_k) = \frac{\sqrt{S_h(f_k)}}{\mathcal{D}_{\text{CR}_i(k)}^{90\%}}, \quad (13)$$

where $\text{CR}_i(k)$ is the significance bin of the loudest candidate of the k th band and $S_h(f_k)$ the power spectral density of the data (measured in $1/\sqrt{\text{Hz}}$). The values of the sensitivity depths range between $\mathcal{D}_{\text{CR}_6}^{90\%} \approx 33(1/\sqrt{\text{Hz}})$ and $\mathcal{D}_{\text{CR}_0}^{90\%} \approx 37(1/\sqrt{\text{Hz}})$. The uncertainties on the upper limit values introduced by this procedure are $\approx 10\%$ of the nominal upper limit value. We represent this uncertainty as a shaded region around the upper limit values in Fig. 9. The upper limit values are also provided in tabular form in the

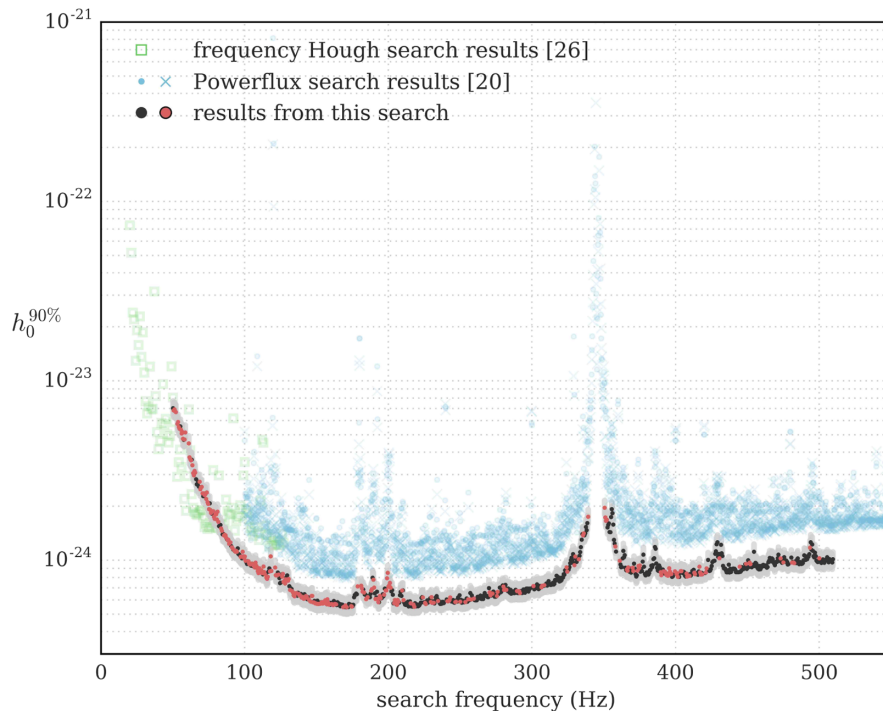


FIG. 9. 90% confidence upper limits on the gravitational wave amplitude of signals with frequency within half-Hz bands, from the entire sky and within the spin-down range of the search. The light red markers denote half-Hz bands where the upper limit value does not hold for all frequencies in that interval. A list of the excluded frequencies is given in the Appendix. Although not obvious from the figure, due to the quality of the data we were not able to analyze the data in some half-Hz bands, so there are some points missing in the plot. For reference we also plot the upper limit results from two searches: one on the same data (Powerflux) [2] and on contemporary data from the Virgo detector (frequency Hough) [4]. The Powerflux points are obtained by rescaling the best (crosses) and worst-case (dots) upper limit values as explained in the text. It should be noted that the Powerflux upper limits are set at 95% rather than 90% but refer to 0.25 Hz bands rather than half-Hz.

Appendix in Table II. We do not set upper limits in half-Hz bands where the results are entirely produced with fake data inserted by the cleaning procedure described in Sec. II. Upper limits for such bands will not appear in Table II nor in Fig. 9. There also exist 50 mHz bands that include contributions from fake data as a result of the cleaning procedure or that have been excluded from the analysis because they were marked as disturbed by the visual inspection procedure described in Sec. III B. We mark the half-Hz bands which host these 50 mHz bands with a different colour (light red) in Fig. 9. In Table IV in the Appendix we provide a complete list of such 50-mHz bands because the upper limit values do not apply to those 50-mHz bands. Finally we note that, due to the cleaning procedure, there exist signal frequency bands where the search results *might* have contributions from fake data. We list these signal-frequency ranges in Table V. For completeness this table also contains the cleaned bands of Table IV, under the column header “all fake data”.

V. CONCLUSIONS

Our upper limits are the tightest ever placed for this set of target signals. The smallest value of the GW amplitude upper limit is 5.5×10^{-25} in the band 170.5–171 Hz. Figure 9 shows the upper limit values as a function of search frequency. We also show the upper limits from [2], another all-sky search on S6 data, rescaled according to [23] to enable a direct comparison with ours. Under the assumption that the sources are uniformly distributed in space, our search probes a volume in space a few times larger than that of [2]. It should however be noted that [2]

examines a much broader parameter space than the one presented here. The Virgo VSR2 and VSR4 science runs were contemporary to the S6 run and more sensitive at low frequency with respect to LIGO. The Virgo data were analyzed in search of continuous signals from the whole sky in the frequency range 20–128 Hz and a narrower spin-down range than that covered here, with $|\dot{f}| \leq 10^{-10}$ Hz/s [4]. Our sensitivity is comparable to that achieved by that search and improves on it above 80 Hz.

Following [24], we define the fraction x of the spin-down rotational energy emitted in gravitational waves. The star’s ellipticity necessary to sustain such emission is

$$\epsilon(f, x\dot{f}) = \sqrt{\frac{5c^5}{32\pi^4 G} \frac{x\dot{f}}{I f^5}}, \quad (14)$$

where c is the speed of light, G is the gravitational constant, f is the GW frequency and I the principal moment of inertia of the star. Correspondingly, $x\dot{f}$ is the spin-down rate that accounts for the emission of GWs, and this is why we refer to it as the GW spin-down. The gravitational wave amplitude h_0 at the detector coming from a GW source like that of Eq. (14), at a distance D from Earth is

$$h_0(f, x\dot{f}, D) = \frac{1}{D} \sqrt{\frac{5GI}{2c^3} \frac{x\dot{f}}{f}}. \quad (15)$$

Based on this last equation, we can use our GW amplitude upper limits to bound the minimum distance for compact objects emitting continuous gravitational waves under different assumptions on the object’s ellipticity (i.e.

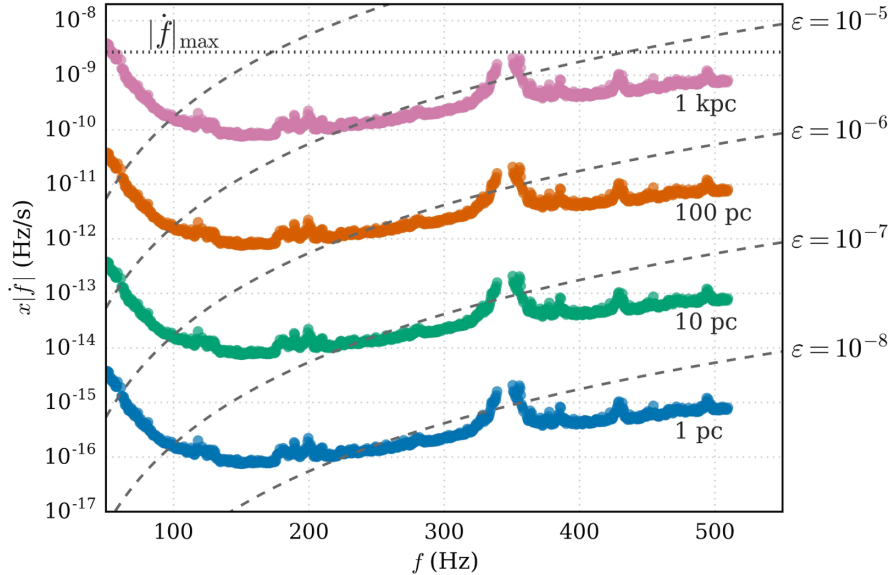


FIG. 10. Gravitational wave amplitude upper limits recast as curves in the $f - |x\dot{f}|$ plane for sources at given distances and having assumed $I = 10^{38}$ kg m². f is the signal frequency and $|x\dot{f}|$ is the gravitational-wave spin-down, i.e. the fraction of the actual spin-down that accounts for the rotational energy loss due to GW emission. Superimposed are curves of constant ellipticity $\epsilon(f, \dot{f}|I = 10^{38}$ kg m²). The dotted line at $|\dot{f}|_{\max}$ indicates the maximum magnitude of searched spin-down.

gravitational wave spin-down). This is shown in Fig. 10. We find that for most frequencies above 230 Hz our upper limits exclude compact objects with ellipticities of $10^{-6} \sqrt{\frac{10^{38} \text{ kg m}^2}{I}}$ (corresponding to GW spin-downs between 10^{-12} Hz/s and 10^{-11} Hz/s) within 100 pc of Earth. Both the ellipticity and the distance ranges span absolutely plausible values and could not have been excluded with other measurements.

We expect the methodology used in this search to serve as a template for the assessment of Einstein@Home run results in the future, for example the next Einstein@Home run, using advanced LIGO data that is being processed as this paper is written. Results of searches for continuous wave signals could also be mined further, probing sub-threshold candidates with a hierarchical series of follow-up searches. This is not the topic of this paper and might be pursued in a forthcoming publication.

ACKNOWLEDGMENTS

The authors gratefully acknowledge the support of the Einstein@Home volunteers, of the United States National Science Foundation for the construction and operation of the LIGO Laboratory, the Science and Technology Facilities Council of the United Kingdom,

the Max-Planck-Society, and the State of Niedersachsen/Germany for support of the construction and operation of the GEO600 detector, and the Italian Istituto Nazionale di Fisica Nucleare and the French Centre National de la Recherche Scientifique for the construction and operation of the Virgo detector. The authors also gratefully acknowledge the support of the research by these agencies and by the Australian Research Council, the International Science Linkages program of the Commonwealth of Australia, the Council of Scientific and Industrial Research of India, the Istituto Nazionale di Fisica Nucleare of Italy, the Spanish Ministerio de Educación y Ciencia, the Conselleria d'Economia Hisenda i Innovació of the Govern de les Illes Balears, the Foundation for Fundamental Research on Matter supported by the Netherlands Organization for Scientific Research, the Polish Ministry of Science and Higher Education, the FOCUS Programme of Foundation for Polish Science, the Royal Society, the Scottish Funding Council, the Scottish Universities Physics Alliance, The National Aeronautics and Space Administration, the Carnegie Trust, the Leverhulme Trust, the David and Lucile Packard Foundation, the Research Corporation, and the Alfred P. Sloan Foundation.

This document has been assigned LIGO Laboratory document No. LIGO-P1600156-v22.

APPENDIX: TABULAR DATA

1. Upper limit values

TABLE II. First frequency of each half Hz signal frequency band in which we set upper limits and upper limit value for that band.

f (in Hz)	$h_0^{90\%} \times 10^{25}$	f (in Hz)	$h_0^{90\%} \times 10^{25}$	f (in Hz)	$h_0^{90\%} \times 10^{25}$	f (in Hz)	$h_0^{90\%} \times 10^{25}$
50.063	70.3 ± 12.8	50.563	68.4 ± 12.5	51.063	69.3 ± 12.6	51.563	67.5 ± 12.4
52.063	66.9 ± 12.2	53.063	57.6 ± 10.5	53.563	58.9 ± 10.9	54.063	55.3 ± 10.1
54.563	54.0 ± 9.9	55.063	55.7 ± 10.2	55.563	53.3 ± 9.8	56.063	50.9 ± 9.3
56.563	51.8 ± 9.5	57.063	47.5 ± 8.7	57.563	46.9 ± 8.6	58.063	47.1 ± 8.6
58.563	51.5 ± 9.4	61.063	44.8 ± 8.2	61.563	37.4 ± 6.9	62.063	36.5 ± 6.7
62.563	36.0 ± 6.6	63.063	36.3 ± 6.6	63.563	33.8 ± 6.2	64.063	30.6 ± 5.6
64.563	29.8 ± 5.4	65.063	31.5 ± 5.9	65.563	30.8 ± 5.7	66.063	28.3 ± 5.2
66.563	26.5 ± 4.8	67.063	26.5 ± 4.9	67.563	27.3 ± 5.0	68.063	25.7 ± 4.7
68.563	27.4 ± 5.0	69.063	24.8 ± 4.5	69.563	25.5 ± 4.7	70.063	25.7 ± 4.7
70.563	23.6 ± 4.3	71.063	22.8 ± 4.2	71.563	23.6 ± 4.3	72.063	23.1 ± 4.2
72.563	23.3 ± 4.2	73.063	22.0 ± 4.0	73.563	23.9 ± 4.5	74.063	21.1 ± 3.8
74.563	20.6 ± 3.8	75.063	19.3 ± 3.5	75.563	20.8 ± 3.8	76.063	19.0 ± 3.5
76.563	18.3 ± 3.4	77.063	18.1 ± 3.3	77.563	18.5 ± 3.4	78.063	18.8 ± 3.4
78.563	17.4 ± 3.2	79.063	17.0 ± 3.1	79.563	18.1 ± 3.3	80.063	18.0 ± 3.3
80.563	16.9 ± 3.1	81.063	18.7 ± 3.4	81.563	16.3 ± 3.0	82.063	15.5 ± 2.8
82.563	15.4 ± 2.8	83.063	15.7 ± 2.9	83.563	15.0 ± 2.8	84.063	14.6 ± 2.7
84.563	13.9 ± 2.5	85.063	14.0 ± 2.6	85.563	13.7 ± 2.5	86.063	13.9 ± 2.5
86.563	13.8 ± 2.5	87.063	13.3 ± 2.4	87.563	13.1 ± 2.4	88.063	12.9 ± 2.4
88.563	13.0 ± 2.4	89.063	12.4 ± 2.3	89.563	12.3 ± 2.3	90.063	12.6 ± 2.3

(Table continued)

TABLE II. (Continued)

f (in Hz)	$h_0^{90\%} \times 10^{25}$	f (in Hz)	$h_0^{90\%} \times 10^{25}$	f (in Hz)	$h_0^{90\%} \times 10^{25}$	f (in Hz)	$h_0^{90\%} \times 10^{25}$
90.563	12.0 ± 2.2	91.063	11.8 ± 2.2	91.563	11.6 ± 2.1	92.063	11.4 ± 2.1
92.563	11.3 ± 2.1	93.063	11.2 ± 2.1	93.563	11.1 ± 2.0	94.063	11.3 ± 2.1
94.563	11.1 ± 2.0	95.063	11.6 ± 2.2	95.563	10.8 ± 2.0	96.063	10.8 ± 2.0
96.563	10.6 ± 1.9	97.063	10.4 ± 1.9	97.563	10.5 ± 1.9	98.063	10.2 ± 1.9
98.563	11.1 ± 2.1	99.063	10.5 ± 1.9	99.563	10.3 ± 1.9	100.063	10.5 ± 1.9
100.563	9.9 ± 1.8	101.063	9.8 ± 1.8	101.563	9.5 ± 1.7	102.063	9.9 ± 1.8
102.563	9.9 ± 1.8	103.063	9.6 ± 1.8	103.563	9.5 ± 1.7	104.063	9.4 ± 1.7
104.563	9.3 ± 1.7	105.063	9.6 ± 1.8	105.563	9.3 ± 1.7	106.063	9.3 ± 1.7
106.563	9.4 ± 1.7	107.063	9.1 ± 1.7	107.563	9.7 ± 1.8	108.063	9.3 ± 1.7
108.563	9.0 ± 1.7	109.063	8.7 ± 1.6	109.563	8.5 ± 1.5	110.063	9.0 ± 1.7
110.563	8.6 ± 1.6	111.063	8.6 ± 1.6	111.563	8.8 ± 1.6	112.063	8.5 ± 1.5
112.563	8.3 ± 1.5	113.063	9.2 ± 1.7	113.563	8.6 ± 1.6	114.063	8.4 ± 1.5
114.563	8.4 ± 1.6	115.063	8.0 ± 1.5	115.563	7.9 ± 1.4	116.063	8.1 ± 1.5
116.563	8.6 ± 1.6	117.063	9.0 ± 1.7	117.563	8.7 ± 1.6	118.063	10.5 ± 1.9
118.563	8.7 ± 1.6	121.063	9.1 ± 1.7	121.563	8.2 ± 1.5	122.063	8.3 ± 1.5
122.563	8.2 ± 1.5	123.063	8.5 ± 1.6	123.563	8.3 ± 1.5	124.063	8.0 ± 1.4
124.563	7.4 ± 1.4	125.063	7.5 ± 1.4	125.563	8.3 ± 1.5	126.063	8.1 ± 1.5
126.563	8.4 ± 1.5	127.063	7.6 ± 1.4	127.563	7.7 ± 1.4	128.063	7.4 ± 1.4
128.563	7.8 ± 1.4	129.063	8.0 ± 1.5	129.563	8.2 ± 1.5	130.063	7.7 ± 1.4
130.563	7.9 ± 1.4	131.063	7.2 ± 1.3	131.563	6.8 ± 1.2	132.063	7.0 ± 1.3
132.563	6.9 ± 1.3	133.063	6.7 ± 1.2	133.563	6.6 ± 1.2	134.063	6.4 ± 1.2
134.563	6.3 ± 1.2	135.063	6.5 ± 1.2	135.563	6.5 ± 1.2	136.063	6.6 ± 1.2
136.563	6.3 ± 1.2	137.063	6.6 ± 1.2	137.563	6.5 ± 1.2	138.063	6.4 ± 1.2
138.563	6.4 ± 1.2	139.063	6.5 ± 1.2	139.563	6.2 ± 1.1	140.063	6.3 ± 1.1
140.563	6.2 ± 1.1	141.063	6.1 ± 1.1	141.563	6.5 ± 1.2	142.063	6.2 ± 1.1
142.563	6.3 ± 1.2	143.063	6.3 ± 1.1	143.563	6.0 ± 1.1	144.063	6.2 ± 1.1
144.563	6.0 ± 1.1	145.563	5.9 ± 1.1	146.063	5.9 ± 1.1	146.563	6.3 ± 1.2
147.063	6.3 ± 1.2	147.563	5.8 ± 1.1	148.063	5.8 ± 1.1	148.563	5.9 ± 1.1
149.063	5.8 ± 1.1	149.563	5.7 ± 1.0	150.063	5.7 ± 1.0	150.563	6.0 ± 1.1
151.063	5.7 ± 1.0	151.563	5.7 ± 1.0	152.063	5.7 ± 1.1	152.563	5.7 ± 1.0
153.063	5.8 ± 1.1	153.563	5.8 ± 1.1	154.063	5.7 ± 1.0	154.563	5.7 ± 1.1
155.063	5.9 ± 1.1	155.563	5.9 ± 1.1	156.063	6.0 ± 1.1	156.563	6.0 ± 1.1
157.063	5.7 ± 1.0	157.563	6.0 ± 1.1	158.063	5.8 ± 1.1	158.563	5.7 ± 1.0
159.063	5.8 ± 1.1	159.563	5.6 ± 1.0	160.063	5.8 ± 1.1	160.563	5.7 ± 1.0
161.063	5.7 ± 1.0	161.563	5.6 ± 1.0	162.063	5.9 ± 1.1	162.563	5.7 ± 1.0
163.063	5.7 ± 1.0	163.563	5.7 ± 1.0	164.063	5.6 ± 1.0	164.563	5.8 ± 1.1
165.063	5.7 ± 1.0	165.563	5.7 ± 1.0	166.063	5.7 ± 1.0	166.563	5.5 ± 1.0
167.063	5.7 ± 1.0	167.563	5.6 ± 1.0	168.063	5.6 ± 1.0	168.563	5.5 ± 1.0
169.063	5.5 ± 1.0	169.563	5.5 ± 1.0	170.063	5.6 ± 1.0	170.563	5.5 ± 1.0
171.063	5.5 ± 1.0	171.563	5.5 ± 1.0	172.063	5.5 ± 1.0	172.563	5.7 ± 1.0
173.063	5.6 ± 1.0	173.563	5.7 ± 1.0	174.063	5.5 ± 1.0	174.563	5.5 ± 1.0
175.063	5.5 ± 1.0	175.563	5.6 ± 1.0	176.063	6.2 ± 1.1	176.563	6.4 ± 1.2
177.063	6.4 ± 1.2	177.563	6.5 ± 1.2	178.063	6.5 ± 1.2	178.563	7.2 ± 1.3
181.063	7.2 ± 1.3	181.563	7.0 ± 1.3	182.063	6.7 ± 1.2	182.563	6.9 ± 1.3
183.063	6.6 ± 1.2	183.563	6.4 ± 1.2	184.063	6.4 ± 1.2	184.563	6.1 ± 1.1
185.063	6.3 ± 1.2	185.563	6.2 ± 1.1	186.063	6.2 ± 1.1	186.563	6.3 ± 1.2
187.063	6.2 ± 1.1	187.563	6.5 ± 1.2	188.063	6.8 ± 1.2	188.563	6.9 ± 1.3
189.063	8.0 ± 1.5	189.563	7.8 ± 1.4	190.063	7.0 ± 1.3	190.563	6.5 ± 1.2
191.063	6.1 ± 1.1	191.563	6.2 ± 1.1	192.063	6.7 ± 1.3	192.563	6.1 ± 1.1
193.063	5.8 ± 1.1	193.563	5.8 ± 1.1	194.063	6.3 ± 1.2	194.563	6.1 ± 1.1
195.063	6.1 ± 1.1	195.563	6.2 ± 1.1	196.063	6.5 ± 1.2	196.563	6.3 ± 1.2
197.063	6.4 ± 1.2	197.563	6.9 ± 1.3	198.063	6.8 ± 1.2	198.563	6.8 ± 1.2
199.063	7.9 ± 1.4	199.563	8.5 ± 1.6	200.063	7.1 ± 1.3	200.563	7.3 ± 1.3
201.063	7.5 ± 1.4	201.563	7.0 ± 1.3	202.063	6.7 ± 1.2	202.563	6.8 ± 1.2
203.063	6.4 ± 1.2	203.563	5.7 ± 1.1	204.063	5.8 ± 1.1	204.563	6.0 ± 1.1

(Table continued)

TABLE II. (*Continued*)

f (in Hz)	$h_0^{90\%} \times 10^{25}$	f (in Hz)	$h_0^{90\%} \times 10^{25}$	f (in Hz)	$h_0^{90\%} \times 10^{25}$	f (in Hz)	$h_0^{90\%} \times 10^{25}$
205.063	5.8 ± 1.1	205.563	5.7 ± 1.0	206.063	5.6 ± 1.0	206.563	6.0 ± 1.1
207.063	5.9 ± 1.1	207.563	5.8 ± 1.1	208.063	6.4 ± 1.2	208.563	6.7 ± 1.2
209.063	6.3 ± 1.2	209.563	6.8 ± 1.2	210.063	6.8 ± 1.2	210.563	6.0 ± 1.1
211.063	5.8 ± 1.1	211.563	5.7 ± 1.0	212.063	5.6 ± 1.0	212.563	5.8 ± 1.1
213.063	5.7 ± 1.0	213.563	5.9 ± 1.1	214.063	5.5 ± 1.0	214.563	5.8 ± 1.1
215.063	5.9 ± 1.1	215.563	5.8 ± 1.1	216.063	5.5 ± 1.0	216.563	5.5 ± 1.0
217.063	5.5 ± 1.0	217.563	5.7 ± 1.0	218.063	5.5 ± 1.0	218.563	5.8 ± 1.1
219.063	5.5 ± 1.0	219.563	5.7 ± 1.0	220.063	5.7 ± 1.0	220.563	5.5 ± 1.0
221.063	5.6 ± 1.0	221.563	5.6 ± 1.0	222.063	5.7 ± 1.0	222.563	5.8 ± 1.1
223.063	6.2 ± 1.1	223.563	6.2 ± 1.1	224.063	6.2 ± 1.1	224.563	5.8 ± 1.1
225.063	5.8 ± 1.1	225.563	5.8 ± 1.1	226.063	5.7 ± 1.0	226.563	5.7 ± 1.0
227.063	6.0 ± 1.1	227.563	5.8 ± 1.1	228.063	5.9 ± 1.1	228.563	5.9 ± 1.1
229.063	6.1 ± 1.1	229.563	5.9 ± 1.1	230.063	6.2 ± 1.1	230.563	5.8 ± 1.1
231.063	5.9 ± 1.1	231.563	5.8 ± 1.1	232.063	5.7 ± 1.1	232.563	5.9 ± 1.1
233.063	6.2 ± 1.1	233.563	6.3 ± 1.1	234.063	6.1 ± 1.1	234.563	5.9 ± 1.1
235.063	5.9 ± 1.1	235.563	5.8 ± 1.1	236.063	5.7 ± 1.0	236.563	5.7 ± 1.0
237.063	5.7 ± 1.0	237.563	5.9 ± 1.1	238.063	5.9 ± 1.1	238.563	5.8 ± 1.1
240.563	6.0 ± 1.1	241.063	5.9 ± 1.1	241.563	5.9 ± 1.1	242.063	5.9 ± 1.1
242.563	6.0 ± 1.1	243.063	6.2 ± 1.1	243.563	6.0 ± 1.1	244.063	5.9 ± 1.1
244.563	5.9 ± 1.1	245.063	6.0 ± 1.1	245.563	5.8 ± 1.1	246.063	5.8 ± 1.1
246.563	5.8 ± 1.1	247.063	5.9 ± 1.1	247.563	6.0 ± 1.1	248.063	5.9 ± 1.1
248.563	6.2 ± 1.1	249.063	6.1 ± 1.1	249.563	6.4 ± 1.2	250.063	5.9 ± 1.1
250.563	6.0 ± 1.1	251.063	5.8 ± 1.1	251.563	5.9 ± 1.1	252.063	5.9 ± 1.1
252.563	5.8 ± 1.1	253.063	5.8 ± 1.1	253.563	5.8 ± 1.1	254.063	5.9 ± 1.1
254.563	6.1 ± 1.1	255.063	5.9 ± 1.1	255.563	6.1 ± 1.1	256.063	6.0 ± 1.1
256.563	6.0 ± 1.1	257.063	6.6 ± 1.2	257.563	6.0 ± 1.1	258.063	6.4 ± 1.2
258.563	6.2 ± 1.1	259.063	6.1 ± 1.1	259.563	6.1 ± 1.1	260.063	6.0 ± 1.1
260.563	6.0 ± 1.1	261.063	6.0 ± 1.1	261.563	6.0 ± 1.1	262.063	6.3 ± 1.1
262.563	6.1 ± 1.1	263.063	6.2 ± 1.1	263.563	6.2 ± 1.1	264.063	6.3 ± 1.2
264.563	6.1 ± 1.1	265.063	6.1 ± 1.1	265.563	6.3 ± 1.1	266.063	6.1 ± 1.1
266.563	6.4 ± 1.2	267.063	6.6 ± 1.2	267.563	6.3 ± 1.2	268.063	6.4 ± 1.2
268.563	6.3 ± 1.2	269.063	6.2 ± 1.1	269.563	6.2 ± 1.1	270.063	7.0 ± 1.3
270.563	6.6 ± 1.2	271.063	6.4 ± 1.2	271.563	6.3 ± 1.2	272.063	6.6 ± 1.2
272.563	6.5 ± 1.2	273.063	6.7 ± 1.2	273.563	6.5 ± 1.2	274.063	6.2 ± 1.1
274.563	6.3 ± 1.1	275.063	6.3 ± 1.1	275.563	6.3 ± 1.2	276.063	6.7 ± 1.2
276.563	6.5 ± 1.2	277.063	6.6 ± 1.2	277.563	7.0 ± 1.3	278.063	6.6 ± 1.2
278.563	6.7 ± 1.2	279.063	6.8 ± 1.3	279.563	7.2 ± 1.3	280.063	7.1 ± 1.3
280.563	6.8 ± 1.2	281.063	6.9 ± 1.3	281.563	7.3 ± 1.3	282.063	6.8 ± 1.3
282.563	6.9 ± 1.3	283.063	6.7 ± 1.2	283.563	6.9 ± 1.3	284.063	6.6 ± 1.2
284.563	6.6 ± 1.2	285.063	6.8 ± 1.3	285.563	6.5 ± 1.2	286.063	6.7 ± 1.2
286.563	6.6 ± 1.2	287.063	6.7 ± 1.2	287.563	6.5 ± 1.2	288.063	6.6 ± 1.2
288.563	6.8 ± 1.2	289.063	6.6 ± 1.2	289.563	6.7 ± 1.2	290.063	6.6 ± 1.2
290.563	6.6 ± 1.2	291.063	6.7 ± 1.2	291.563	6.6 ± 1.2	292.063	6.7 ± 1.2
292.563	6.6 ± 1.2	293.063	6.6 ± 1.2	293.563	6.8 ± 1.2	294.063	6.9 ± 1.3
294.563	6.6 ± 1.2	295.063	6.6 ± 1.2	295.563	6.9 ± 1.3	296.063	6.9 ± 1.3
296.563	6.7 ± 1.2	297.063	6.9 ± 1.3	297.563	6.7 ± 1.2	298.063	6.9 ± 1.3
298.563	6.9 ± 1.3	300.563	7.1 ± 1.3	301.063	7.2 ± 1.3	301.563	6.9 ± 1.3
302.063	6.9 ± 1.3	302.563	7.1 ± 1.3	303.063	7.1 ± 1.3	303.563	7.3 ± 1.3
304.063	7.2 ± 1.3	304.563	6.9 ± 1.3	305.063	7.0 ± 1.3	305.563	7.2 ± 1.3
306.063	7.1 ± 1.3	306.563	7.1 ± 1.3	307.063	7.2 ± 1.3	307.563	7.2 ± 1.3
308.063	7.2 ± 1.3	308.563	7.3 ± 1.3	309.063	7.2 ± 1.3	309.563	7.3 ± 1.3
310.063	7.4 ± 1.4	310.563	7.2 ± 1.3	311.063	7.5 ± 1.4	311.563	7.6 ± 1.4
312.063	7.4 ± 1.4	312.563	7.3 ± 1.3	313.063	7.3 ± 1.3	313.563	7.3 ± 1.3
314.063	7.3 ± 1.3	314.563	7.5 ± 1.4	315.063	7.3 ± 1.3	315.563	7.4 ± 1.4
316.063	7.8 ± 1.4	316.563	7.7 ± 1.4	317.063	8.2 ± 1.5	317.563	7.8 ± 1.4

(Table continued)

TABLE II. (*Continued*)

f (in Hz)	$h_0^{90\%} \times 10^{25}$	f (in Hz)	$h_0^{90\%} \times 10^{25}$	f (in Hz)	$h_0^{90\%} \times 10^{25}$	f (in Hz)	$h_0^{90\%} \times 10^{25}$
318.063	8.1 ± 1.5	318.563	7.8 ± 1.4	319.063	7.6 ± 1.4	319.563	8.0 ± 1.5
320.063	7.7 ± 1.4	320.563	7.7 ± 1.4	321.063	8.0 ± 1.5	321.563	8.0 ± 1.5
322.063	8.4 ± 1.5	322.563	8.3 ± 1.5	323.063	8.8 ± 1.6	323.563	8.7 ± 1.6
324.063	9.1 ± 1.7	324.563	8.6 ± 1.6	325.063	9.0 ± 1.6	325.563	8.9 ± 1.6
326.063	9.1 ± 1.7	326.563	9.6 ± 1.8	327.063	10.0 ± 1.8	327.563	10.3 ± 1.9
328.063	10.0 ± 1.8	328.563	10.8 ± 2.0	329.063	9.6 ± 1.8	329.563	9.4 ± 1.7
330.063	10.5 ± 1.9	330.563	10.2 ± 1.9	331.063	9.8 ± 1.8	331.563	10.2 ± 1.9
332.063	10.2 ± 1.9	332.563	10.1 ± 1.9	333.063	10.6 ± 1.9	333.563	11.1 ± 2.0
334.063	11.8 ± 2.2	334.563	13.0 ± 2.4	335.063	14.0 ± 2.6	335.563	13.8 ± 2.5
336.063	14.1 ± 2.6	336.563	13.8 ± 2.5	337.063	14.1 ± 2.6	337.563	15.3 ± 2.9
338.063	14.7 ± 2.7	338.563	16.1 ± 2.9	339.063	17.4 ± 3.2	350.563	19.6 ± 3.6
351.063	17.3 ± 3.2	351.563	16.6 ± 3.0	352.063	16.8 ± 3.1	352.563	15.2 ± 2.8
353.063	15.7 ± 2.9	353.563	16.0 ± 2.9	354.063	14.4 ± 2.6	354.563	14.3 ± 2.6
355.063	17.4 ± 3.2	355.563	19.3 ± 3.5	356.063	18.3 ± 3.3	356.563	15.8 ± 2.9
357.063	13.0 ± 2.4	357.563	12.4 ± 2.3	358.063	11.9 ± 2.2	358.563	11.2 ± 2.0
361.063	9.9 ± 1.8	361.563	9.5 ± 1.7	362.063	9.1 ± 1.7	362.563	9.2 ± 1.7
363.063	10.2 ± 1.9	363.563	11.3 ± 2.1	364.063	10.4 ± 1.9	364.563	10.7 ± 2.0
365.063	9.1 ± 1.7	365.563	8.8 ± 1.6	366.063	8.9 ± 1.6	366.563	8.7 ± 1.6
367.063	9.1 ± 1.7	367.563	9.0 ± 1.6	368.063	8.6 ± 1.6	368.563	9.0 ± 1.6
369.063	8.5 ± 1.6	369.563	8.9 ± 1.6	370.063	9.1 ± 1.7	370.563	8.7 ± 1.6
371.063	9.6 ± 1.8	371.563	9.0 ± 1.6	372.063	8.4 ± 1.5	372.563	8.1 ± 1.5
373.063	8.3 ± 1.5	373.563	8.7 ± 1.6	374.063	9.3 ± 1.7	374.563	9.0 ± 1.6
375.063	9.3 ± 1.7	375.563	8.6 ± 1.6	376.063	8.9 ± 1.6	376.563	8.7 ± 1.6
377.063	9.8 ± 1.8	377.563	10.7 ± 2.0	378.063	9.2 ± 1.7	378.563	8.4 ± 1.5
379.063	8.2 ± 1.5	379.563	8.4 ± 1.5	380.063	8.6 ± 1.6	380.563	8.5 ± 1.5
381.063	8.3 ± 1.5	381.563	8.5 ± 1.6	382.063	8.8 ± 1.6	382.563	8.9 ± 1.6
383.063	9.3 ± 1.7	383.563	9.1 ± 1.7	384.063	9.4 ± 1.7	384.563	10.2 ± 1.9
385.063	10.3 ± 1.9	385.563	11.9 ± 2.2	386.063	11.6 ± 2.1	386.563	9.6 ± 1.7
387.063	9.1 ± 1.7	387.563	8.8 ± 1.6	388.063	8.7 ± 1.6	388.563	9.3 ± 1.7
389.063	9.2 ± 1.7	389.563	8.6 ± 1.6	390.063	8.3 ± 1.5	390.563	8.8 ± 1.6
391.063	8.9 ± 1.6	391.563	8.7 ± 1.6	392.063	8.4 ± 1.5	392.563	8.6 ± 1.6
393.063	8.5 ± 1.6	393.563	8.3 ± 1.5	394.063	8.4 ± 1.5	394.563	8.2 ± 1.5
395.063	8.2 ± 1.5	395.563	9.0 ± 1.7	396.063	8.6 ± 1.6	396.563	8.4 ± 1.5
397.063	8.4 ± 1.5	397.563	8.1 ± 1.5	398.063	8.1 ± 1.5	398.563	8.3 ± 1.5
399.063	8.4 ± 1.5	399.563	8.7 ± 1.6	400.563	8.3 ± 1.5	401.063	8.5 ± 1.6
401.563	8.1 ± 1.5	402.063	8.1 ± 1.5	402.563	8.1 ± 1.5	403.063	8.5 ± 1.6
403.563	8.7 ± 1.6	404.063	8.7 ± 1.6	404.563	8.6 ± 1.6	405.063	8.5 ± 1.6
405.563	8.6 ± 1.6	406.063	8.6 ± 1.6	406.563	8.2 ± 1.5	407.063	8.1 ± 1.5
407.563	8.4 ± 1.5	408.063	8.1 ± 1.5	408.563	8.2 ± 1.5	409.063	8.2 ± 1.5
409.563	8.2 ± 1.5	410.063	8.4 ± 1.5	410.563	8.2 ± 1.5	411.063	8.4 ± 1.5
411.563	8.7 ± 1.6	412.063	8.7 ± 1.6	412.563	8.8 ± 1.6	413.063	8.5 ± 1.6
413.563	8.4 ± 1.5	414.063	8.4 ± 1.5	414.563	8.5 ± 1.5	415.063	8.5 ± 1.5
415.563	8.3 ± 1.5	416.063	8.7 ± 1.6	416.563	9.2 ± 1.7	417.063	8.6 ± 1.6
417.563	8.3 ± 1.5	418.063	8.5 ± 1.6	418.563	8.3 ± 1.5	420.563	8.5 ± 1.6
421.063	8.5 ± 1.6	421.563	9.0 ± 1.7	422.063	8.8 ± 1.6	422.563	10.0 ± 1.8
423.063	8.8 ± 1.6	423.563	8.7 ± 1.6	424.063	8.7 ± 1.6	424.563	8.9 ± 1.6
425.063	9.3 ± 1.7	425.563	9.7 ± 1.8	426.063	9.8 ± 1.8	426.563	9.9 ± 1.8
427.063	9.9 ± 1.8	427.563	10.9 ± 2.0	428.063	11.2 ± 2.1	428.563	12.3 ± 2.2
429.063	12.6 ± 2.3	429.563	10.4 ± 1.9	430.063	10.8 ± 2.0	430.563	10.3 ± 1.9
431.063	10.5 ± 1.9	431.563	12.2 ± 2.2	432.063	10.9 ± 2.0	432.563	10.6 ± 1.9
433.063	9.3 ± 1.7	433.563	9.0 ± 1.6	434.063	9.0 ± 1.6	434.563	9.0 ± 1.6
435.063	8.8 ± 1.6	435.563	8.6 ± 1.6	436.063	8.6 ± 1.6	436.563	8.8 ± 1.6
437.063	9.4 ± 1.8	437.563	8.5 ± 1.6	438.063	9.0 ± 1.6	438.563	8.6 ± 1.6
439.063	8.8 ± 1.6	439.563	8.9 ± 1.6	440.063	9.0 ± 1.6	440.563	8.9 ± 1.6
441.063	9.0 ± 1.6	441.563	8.8 ± 1.6	442.063	8.6 ± 1.6	442.563	8.6 ± 1.6

(Table continued)

TABLE II. (*Continued*)

f (in Hz)	$h_0^{90\%} \times 10^{25}$	f (in Hz)	$h_0^{90\%} \times 10^{25}$	f (in Hz)	$h_0^{90\%} \times 10^{25}$	f (in Hz)	$h_0^{90\%} \times 10^{25}$
443.063	8.6 ± 1.6	443.563	8.6 ± 1.6	444.063	8.6 ± 1.6	444.563	9.2 ± 1.7
445.063	8.6 ± 1.6	445.563	8.7 ± 1.6	446.063	9.2 ± 1.7	446.563	9.1 ± 1.7
447.063	8.9 ± 1.6	447.563	9.0 ± 1.7	448.063	9.0 ± 1.6	448.563	9.5 ± 1.7
449.063	9.5 ± 1.8	449.563	8.9 ± 1.6	450.063	9.1 ± 1.7	450.563	10.0 ± 1.8
451.063	9.2 ± 1.7	451.563	9.7 ± 1.8	452.063	9.5 ± 1.7	452.563	9.2 ± 1.7
453.063	9.1 ± 1.7	453.563	9.4 ± 1.7	454.063	9.5 ± 1.7	454.563	11.1 ± 2.1
455.063	9.3 ± 1.7	455.563	9.7 ± 1.8	456.063	9.6 ± 1.8	456.563	9.4 ± 1.7
457.063	9.0 ± 1.7	457.563	8.9 ± 1.6	458.063	8.9 ± 1.6	458.563	9.3 ± 1.7
459.063	8.9 ± 1.6	459.563	9.1 ± 1.7	460.063	9.3 ± 1.7	460.563	9.4 ± 1.7
461.063	9.4 ± 1.7	461.563	9.3 ± 1.7	462.063	9.3 ± 1.7	462.563	9.3 ± 1.7
463.063	9.4 ± 1.7	463.563	9.1 ± 1.7	464.063	9.2 ± 1.7	464.563	9.7 ± 1.8
465.063	9.9 ± 1.8	465.563	10.3 ± 1.9	466.063	9.9 ± 1.8	466.563	9.8 ± 1.8
467.063	10.2 ± 1.9	467.563	10.1 ± 1.9	468.063	9.8 ± 1.8	468.563	9.6 ± 1.8
469.063	9.4 ± 1.7	469.563	9.7 ± 1.8	470.063	9.8 ± 1.8	470.563	9.8 ± 1.8
471.063	10.3 ± 1.9	471.563	10.7 ± 2.0	472.063	10.2 ± 1.9	472.563	9.9 ± 1.8
473.063	10.2 ± 1.9	473.563	9.9 ± 1.8	474.063	9.7 ± 1.8	474.563	10.0 ± 1.8
475.063	9.7 ± 1.8	475.563	10.4 ± 1.9	476.063	10.0 ± 1.8	476.563	9.8 ± 1.8
477.063	10.0 ± 1.8	477.563	9.8 ± 1.8	478.063	9.5 ± 1.7	478.563	9.5 ± 1.7
480.563	10.3 ± 1.9	481.063	9.7 ± 1.8	481.563	9.8 ± 1.8	482.063	9.7 ± 1.8
482.563	9.6 ± 1.8	483.063	9.7 ± 1.8	483.563	9.9 ± 1.8	484.063	9.6 ± 1.8
484.563	10.1 ± 1.8	485.063	10.2 ± 1.9	485.563	9.7 ± 1.8	486.063	9.5 ± 1.7
486.563	9.8 ± 1.8	487.063	9.5 ± 1.7	487.563	9.5 ± 1.7	488.063	9.5 ± 1.7
488.563	9.7 ± 1.8	489.063	10.0 ± 1.8	489.563	10.7 ± 1.9	490.063	10.6 ± 1.9
490.563	10.0 ± 1.8	491.063	10.3 ± 1.9	491.563	10.1 ± 1.9	492.063	10.5 ± 1.9
492.563	10.5 ± 1.9	493.063	10.8 ± 2.0	493.563	11.7 ± 2.1	494.063	12.6 ± 2.3
494.563	11.4 ± 2.1	495.063	12.3 ± 2.2	495.563	11.3 ± 2.1	496.063	10.5 ± 1.9
496.563	10.4 ± 1.9	497.063	11.0 ± 2.1	497.563	10.5 ± 1.9	498.063	10.0 ± 1.8
498.563	9.8 ± 1.8	499.063	9.7 ± 1.8	499.563	9.9 ± 1.8	500.063	10.2 ± 1.9
500.563	10.0 ± 1.8	501.063	9.9 ± 1.8	501.563	9.7 ± 1.8	502.063	9.9 ± 1.8
502.563	10.1 ± 1.9	503.063	9.7 ± 1.8	503.563	9.7 ± 1.8	504.063	10.0 ± 1.8
504.563	10.1 ± 1.8	505.063	10.2 ± 1.9	505.563	10.4 ± 1.9	506.063	10.0 ± 1.8
506.563	9.7 ± 1.8	507.063	10.1 ± 1.9	507.563	9.9 ± 1.8	508.063	9.9 ± 1.8

2. Cleaned-out frequency bins

TABLE III. Instrumental lines identified and “cleaned” before the Einstein@Home runs. The different columns represent: (I) the source of the line, (II) the central frequency of the instrumental line, (III) the number of harmonics; (IV) low-frequency-side (LFS) of the knockout band, (V) high-frequency-side (HFS) of the knockout band; (VI) the interferometer where the instrumental lines were identified. Note that when there are higher harmonics, the knockout band width remains constant.

Cause	f_L (Hz)	Harmonics	LFS (Hz)	HFS (Hz)	IFO
Mains	60	8	1	1	L,H
Wire	345	1	5	5	L
Wire	346	1	4	4	H
Electronic	85.8	1	0.01	0.01	H
Electronic	89.9	1	0.06	0.06	H
Electronic	93.29	1	0.015	0.015	L
Electronic	93.05	1	0.01	0.01	H
Electronic	93.25	1	0.01	0.01	H
Electronic	96.71	1	0.015	0.015	L
Electronic	139.94	1	0.02	0.02	L
Electronic	139.95	1	0.01	0.01	H

(*Table continued*)

TABLE III. (Continued)

Cause	f_L (Hz)	Harmonics	LFS (Hz)	HFS (Hz)	IFO
Electronic	145.06	1	0.02	0.02	L
Electronic	164.52	1	0.01	0.01	H
Electronic	186.59	1	0.025	0.025	L
Electronic	193.42	1	0.025	0.025	L
Electronic	233.23	1	0.05	0.05	L
Electronic	241.78	1	0.07	0.07	L
Electronic	329.58	1	0.02	0.01	H
Electronic	329.86	1	0.01	0.02	H
Violin mode	329.32	1	0.11	0.11	L
Violin mode	329.70	1	0.3	0.3	H
Violin mode	335.53	1	0.28	0.28	L
CPU line	54.496	1	0.0006	0.0006	L,H
CPU line	108.992	1	0.0006	0.0006	L,H
Sideband comb	140.4100	1	0.0006	0.0006	H
Sideband comb	166.1205	1	0.0006	0.0006	H
Sideband comb	191.8322	1	0.0006	0.0006	H
Sideband comb	217.5428	1	0.0006	0.0006	H
Sideband comb	243.2539	1	0.0006	0.0006	H
Sideband comb	268.9650	1	0.0006	0.0006	H
Sideband comb	294.6756	1	0.0006	0.0006	H
Sideband comb	320.3867	1	0.0006	0.0006	H
Sideband comb	346.0972	1	0.0006	0.0006	H
Sideband comb	371.8077	1	0.0006	0.0006	H
Sideband comb	383.6639	1	0.0006	0.0006	H
Sideband comb	397.5194	1	0.0006	0.0006	H
Sideband comb	409.3705	1	0.0006	0.0006	H
Sideband comb	423.2306	1	0.0006	0.0006	H
Sideband comb	435.0861	1	0.0006	0.0006	H
Sideband comb	460.7967	1	0.0006	0.0006	H
Sideband comb	486.5078	1	0.0006	0.0006	H
1 Hz comb	1	2000	0.0006	0.0006	L,H
2 Hz comb	52	1	0.0006	0.0006	L,H
2 Hz comb	64	1	0.0006	0.0006	L,H
2 Hz comb	68	1	0.0006	0.0006	L,H
2 Hz comb	76	1	0.0006	0.0006	L,H
2 Hz comb	80	1	0.0006	0.0006	L,H
2 Hz comb	82	1	0.0006	0.0006	L,H
2 Hz comb	90	1	0.0006	0.0006	L,H
2 Hz comb	96	1	0.0006	0.0006	L,H
2 Hz comb	98	1	0.0006	0.0006	L,H
2 Hz comb	102	1	0.0006	0.0006	L,H
2 Hz comb	109	1	0.0006	0.0006	L,H
2 Hz comb	110	1	0.0006	0.0006	L,H
2 Hz comb	111	1	0.0006	0.0006	L,H
2 Hz comb	112	1	0.0006	0.0006	L,H
2 Hz comb	116	1	0.0006	0.0006	L,H
2 Hz comb	120	1	0.0006	0.0006	L,H
2 Hz comb	124	1	0.0006	0.0006	L,H
2 Hz comb	128	1	0.0006	0.0006	L,H
2 Hz comb	132	1	0.0006	0.0006	L,H
2 Hz comb	138	1	0.0006	0.0006	L,H
2 Hz comb	140	1	0.0006	0.0006	L,H
2 Hz comb	142	1	0.0006	0.0006	L,H
2 Hz comb	144	1	0.0006	0.0006	L,H
2 Hz comb	150	1	0.0006	0.0006	L,H

(Table continued)

TABLE III. (*Continued*)

Cause	f_L (Hz)	Harmonics	LFS (Hz)	HFS (Hz)	IFO
2 Hz comb	158	1	0.0006	0.0006	L,H
2 Hz comb	154	1	0.0006	0.0006	L,H
2 Hz comb	162	1	0.0006	0.0006	L,H
2 Hz comb	166	1	0.0006	0.0006	L,H
2 Hz comb	168	1	0.0006	0.0006	L,H
2 Hz comb	170	1	0.0006	0.0006	L,H
2 Hz comb	172	1	0.0006	0.0006	L,H
2 Hz comb	174	1	0.0006	0.0006	L,H
2 Hz comb	176	1	0.0006	0.0006	L,H
2 Hz comb	178	1	0.0006	0.0006	L,H
2 Hz comb	184	1	0.0006	0.0006	L,H
2 Hz comb	188	1	0.0006	0.0006	L,H
2 Hz comb	192	1	0.0006	0.0006	L,H
2 Hz comb	196	1	0.0006	0.0006	L,H
2 Hz comb	204	1	0.0006	0.0006	L,H
2 Hz comb	206	1	0.0006	0.0006	L,H
2 Hz comb	214	1	0.0006	0.0006	L,H
2 Hz comb	216	1	0.0006	0.0006	L,H
2 Hz comb	218	1	0.0006	0.0006	L,H
2 Hz comb	221	1	0.0006	0.0006	L,H
2 Hz comb	222	1	0.0006	0.0006	L,H
2 Hz comb	226	1	0.0006	0.0006	L,H
2 Hz comb	234	1	0.0006	0.0006	L,H
2 Hz comb	236	1	0.0006	0.0006	L,H
2 Hz comb	242	1	0.0006	0.0006	L,H
2 Hz comb	244	1	0.0006	0.0006	L,H
2 Hz comb	248	1	0.0006	0.0006	L,H
2 Hz comb	252	1	0.0006	0.0006	L,H
2 Hz comb	254	1	0.0006	0.0006	L,H
2 Hz comb	256	1	0.0006	0.0006	L,H
2 Hz comb	260	1	0.0006	0.0006	L,H
2 Hz comb	262	1	0.0006	0.0006	L,H
2 Hz comb	264	1	0.0006	0.0006	L,H
2 Hz comb	266	1	0.0006	0.0006	L,H
2 Hz comb	268	1	0.0006	0.0006	L,H
2 Hz comb	270	1	0.0006	0.0006	L,H
2 Hz comb	274	1	0.0006	0.0006	L,H
2 Hz comb	278	1	0.0006	0.0006	L,H
2 Hz comb	280	1	0.0006	0.0006	L,H
2 Hz comb	282	1	0.0006	0.0006	L,H
2 Hz comb	286	1	0.0006	0.0006	L,H
2 Hz comb	290	1	0.0006	0.0006	L,H
2 Hz comb	298	1	0.0006	0.0006	L,H
2 Hz comb	308	1	0.0006	0.0006	L,H
2 Hz comb	312	1	0.0006	0.0006	L,H
2 Hz comb	316	1	0.0006	0.0006	L,H
2 Hz comb	320	1	0.0006	0.0006	L,H
2 Hz comb	334	1	0.0006	0.0006	L,H
2 Hz comb	372	1	0.0006	0.0006	L,H
2 Hz comb	376	1	0.0006	0.0006	L,H
2 Hz comb	380	1	0.0006	0.0006	L,H
2 Hz comb	384	1	0.0006	0.0006	L,H
2 Hz comb	394	1	0.0006	0.0006	L,H
2 Hz comb	402	1	0.0006	0.0006	L,H
2 Hz comb	410	1	0.0006	0.0006	L,H

(Table continued)

TABLE III. (Continued)

Cause	f_L (Hz)	Harmonics	LFS (Hz)	HFS (Hz)	IFO
2 Hz comb	414	1	0.0006	0.0006	L,H
2 Hz comb	418	1	0.0006	0.0006	L,H
2 Hz comb	422	1	0.0006	0.0006	L,H
2 Hz comb	430	1	0.0006	0.0006	L,H
2 Hz comb	432	1	0.0006	0.0006	L,H
2 Hz comb	435	1	0.0006	0.0006	L,H
2 Hz comb	440	1	0.0006	0.0006	L,H
2 Hz comb	448	1	0.0006	0.0006	L,H
2 Hz comb	462	1	0.0006	0.0006	L,H
2 Hz comb	466	1	0.0006	0.0006	L,H
2 Hz comb	468	1	0.0006	0.0006	L,H
2 Hz comb	470	1	0.0006	0.0006	L,H
2 Hz comb	474	1	0.0006	0.0006	L,H
2 Hz comb	482	1	0.0006	0.0006	L,H
2 Hz comb	488	1	0.0006	0.0006	L,H
2 Hz comb	496	1	0.0006	0.0006	L,H
2 Hz comb	500	1	0.0006	0.0006	L,H
2 Hz comb	504	1	0.0006	0.0006	L,H
2 Hz comb	508	1	0.0006	0.0006	L,H
Digital	55.8	1	0.05	0.05	H
Digital	56.875	1	0.005	0.005	H
Digital	58.625	1	0.005	0.005	H
Digital	69.	1	0.05	0.05	H
Digital	85.375	1	0.005	0.005	H
Digital	113.75	1	0.01	0.01	H
Digital	140.24	1	0.01	0.01	H
Digital	153.75	1	0.05	0.05	H
Digital	158.0	1	0.05	0.05	H
Digital	199.57	1	0.01	0.01	H
Digital	210.36	1	0.01	0.01	H
Digital	373.5	1	0.05	0.05	H
Digital	392.2	1	0.0006	0.0006	L,H
Digital	399.3	1	0.0006	0.0006	L
Digital	401.5	1	0.05	0.05	H

3. 50 mHz signal-frequency bands that did not contribute to results

TABLE IV. Signal frequency ranges where the results might have contributions from fake data. When the results are entirely due to artificial data, the band is listed in the “all fake data” column; bands where the results comprise contributions from both fake and real data are listed in the other three columns. The “mixed, left” and “mixed, right” columns are populated only when there is a matching “all fake data” entry, which highlights the same physical cause for the fake data, i.e., the cleaning. The “mixed, isolated” column lists isolated ranges of mixed data. The list of input data frequencies where the data was substituted with artificial noise are given in Table I.

Line type	Mixed, isolated		Mixed, left		All fake data		Mixed, right		Detector
1 Hz	50.9648	51.0352							L,H
1 Hz, 2 Hz	51.9647	52.0353							L,H
1 Hz	52.9646	53.0354							L,H
1 Hz	53.9645	54.0355							L,H
CPU	54.4605	54.5315							L,H
1 Hz	54.9644	55.0356							L,H
D			55.715	55.785	55.785	55.815	55.815	55.885	H
1 Hz	55.9643	56.0357							L,H

(Table continued)

TABLE IV. (*Continued*)

Line type	Mixed, isolated		Mixed, left		All fake data		Mixed, right		Detector
D	56.8348	56.9152							H
1 Hz	56.9642	57.0358							L,H
1 Hz	57.9641	58.0359							L,H
D	58.5847	58.6653							H
1 Hz, M			58.964	59.0348	59.0348	60.965	60.965	61.0362	L,H
1 Hz	61.9637	62.0363							L,H
1 Hz	62.9636	63.0364							L,H
1 Hz, 2 Hz	63.9635	64.0365							L,H
1 Hz	64.9634	65.0366							L,H
1 Hz	65.9633	66.0367							L,H
1 Hz	66.9632	67.0368							L,H
1 Hz, 2 Hz	67.9631	68.0369							L,H
1 Hz, D			68.9136	68.9864	68.9864	69.0136	69.0136	69.0864	H
1 Hz	68.963	69.037							L
1 Hz	69.9629	70.0371							L,H
1 Hz	70.9628	71.0372							L,H
1 Hz	71.9627	72.0373							L,H
1 Hz	72.9626	73.0374							L,H
1 Hz	73.9625	74.0375							L,H
1 Hz	74.9624	75.0376							L,H
1 Hz, 2 Hz	75.9623	76.0377							L,H
1 Hz	76.9622	77.0378							L,H
1 Hz	77.9621	78.0379							L,H
1 Hz	78.962	79.038							L,H
1 Hz, 2 Hz	79.9619	80.0381							L,H
1 Hz	80.9618	81.0382							L,H
1 Hz, 2 Hz	81.9617	82.0383							L,H
1 Hz	82.9616	83.0384							L,H
1 Hz	83.9615	84.0385							L,H
1 Hz	84.9614	85.0386							L,H
D	85.332	85.418							H
E	85.752	85.848							H
1 Hz	85.9613	86.0387							L,H
1 Hz	86.9612	87.0388							L,H
1 Hz	87.9611	88.0389							L,H
1 Hz	88.961	89.039							L,H
E			89.8016	89.8784	89.8784	89.9215	89.9215	89.9985	H
1 Hz, 2 Hz	89.9609	90.0391							L,H
1 Hz	90.9608	91.0392							L,H
1 Hz	91.9607	92.0393							L,H
1 Hz	92.9606	93.0394							L,H
E	93.0012	93.0988							H
E	93.2012	93.2988							H
E	93.2362	93.3438							L
1 Hz	93.9605	94.0395							L,H
1 Hz	94.9604	95.0396							L,H
1 Hz, 2 Hz	95.9603	96.0397							L,H
E	96.6559	96.7641							L
1 Hz	96.9602	97.0398							L,H
1 Hz, 2 Hz	97.9601	98.0399							L,H
1 Hz	98.96	99.04							L,H
1 Hz	99.9599	100.0401							L,H
1 Hz	100.9598	101.0402							L,H
1 Hz, 2 Hz	101.9597	102.0403							L,H
1 Hz	102.9596	103.0404							L,H

(Table continued)

TABLE IV. (*Continued*)

Line type	Mixed, isolated		Mixed, left		All fake data		Mixed, right		Detector
1 Hz	103.9595	104.0405							L,H
1 Hz	104.9594	105.0406							L,H
1 Hz	105.9593	106.0407							L,H
1 Hz	106.9592	107.0408							L,H
1 Hz	107.9591	108.0409							L,H
CPU	108.951	109.033							L,H
1 Hz, 2 Hz	108.959	109.041							L,H
1 Hz, 2 Hz	109.9589	110.0411							L,H
1 Hz, 2 Hz	110.9588	111.0412							L,H
1 Hz, 2 Hz	111.9587	112.0413							L,H
1 Hz	112.9586	113.0414							L,H
D	113.6992	113.8008							H
1 Hz	113.9585	114.0415							L,H
1 Hz	114.9584	115.0416							L,H
1 Hz, 2 Hz	115.9583	116.0417							L,H
1 Hz	116.9582	117.0418							L,H
1 Hz	117.9581	118.0419							L,H
1 Hz, 2 Hz, M			118.958	119.0408	119.0408	120.959	120.959	121.0422	L,H
1 Hz	121.9577	122.0423							L,H
1 Hz	122.9576	123.0424							L,H
1 Hz, 2 Hz	123.9575	124.0425							L,H
1 Hz	124.9574	125.0426							L,H
1 Hz	125.9573	126.0427							L,H
1 Hz	126.9572	127.0428							L,H
1 Hz, 2 Hz	127.9571	128.0429							L,H
1 Hz	128.957	129.043							L,H
1 Hz	129.9569	130.0431							L,H
1 Hz	130.9568	131.0432							L,H
1 Hz, 2 Hz	131.9567	132.0433							L,H
1 Hz	132.9566	133.0434							L,H
1 Hz	133.9565	134.0435							L,H
1 Hz	134.9564	135.0436							L,H
1 Hz	135.9563	136.0437							L,H
1 Hz	136.9562	137.0438							L,H
1 Hz, 2 Hz	137.9561	138.0439							L,H
1 Hz	138.956	139.044							L,H
E	139.8765	140.0035							L
E	139.8965	140.0035							H
1 Hz, 2 Hz	139.9559	140.0441							L,H
D	140.1865	140.2935							H
SB	140.3659	140.4541							H
1 Hz	140.9558	141.0442							L,H
1 Hz, 2 Hz	141.9557	142.0443							L,H
1 Hz	142.9556	143.0444							L,H
1 Hz, 2 Hz	143.9555	144.0445							L,H
1 Hz	144.9554	145.0446							L,H
E	144.996	145.124							L
1 Hz	145.9553	146.0447							L,H
1 Hz	146.9552	147.0448							L,H
1 Hz	147.9551	148.0449							L,H
1 Hz	148.955	149.045							L,H
1 Hz, 2 Hz	149.9549	150.0451							L,H
1 Hz	150.9548	151.0452							L,H
1 Hz	151.9547	152.0453							L,H
1 Hz	152.9546	153.0454							L,H

(Table continued)

TABLE IV. (*Continued*)

Line type	Mixed, isolated		Mixed, left		All fake data		Mixed, right		Detector
D			153.6552	153.7448	153.7448	153.7552	153.7552	153.8448	H
1 Hz, 2 Hz	153.9545	154.0455							L,H
1 Hz	154.9544	155.0456							L,H
1 Hz	155.9543	156.0457							L,H
1 Hz	156.9542	157.0458							L,H
1 Hz, 2 Hz, D			157.9047	157.9953	157.9953	158.0047	158.0047	158.0953	H
1 Hz, 2 Hz	157.9541	158.0459							L
1 Hz	158.954	159.046							L,H
1 Hz	159.9539	160.0461							L,H
1 Hz	160.9538	161.0462							L,H
1 Hz, 2 Hz	161.9537	162.0463							L,H
1 Hz	162.9536	163.0464							L,H
1 Hz	163.9535	164.0465							L,H
E	164.4641	164.5759							H
1 Hz	164.9534	165.0466							L,H
1 Hz, 2 Hz	165.9533	166.0467							L,H
SB	166.0738	166.1672							H
1 Hz	166.9532	167.0468							L,H
1 Hz, 2 Hz	167.9531	168.0469							L,H
1 Hz	168.953	169.047							L,H
1 Hz, 2 Hz	169.9529	170.0471							L,H
1 Hz	170.9528	171.0472							L,H
1 Hz, 2 Hz	171.9527	172.0473							L,H
1 Hz	172.9526	173.0474							L,H
1 Hz, 2 Hz	173.9525	174.0475							L,H
1 Hz	174.9524	175.0476							L,H
1 Hz, 2 Hz	175.9523	176.0477							L,H
1 Hz	176.9522	177.0478							L,H
1 Hz, 2 Hz	177.9521	178.0479							L,H
1 Hz, M			178.952	179.0468	179.0468	180.953	180.953	181.0482	L,H
1 Hz	181.9517	182.0483							L,H
1 Hz	182.9516	183.0484							L,H
1 Hz, 2 Hz	183.9515	184.0485							L,H
1 Hz	184.9514	185.0486							L,H
1 Hz	185.9513	186.0487							L,H
E	186.5169	186.6631							L
1 Hz	186.9512	187.0488							L,H
1 Hz, 2 Hz	187.9511	188.0489							L,H
1 Hz	188.951	189.049							L,H
1 Hz	189.9509	190.0491							L,H
1 Hz	190.9508	191.0492							L,H
SB	191.783	191.8814							H
1 Hz, 2 Hz	191.9507	192.0493							L,H
1 Hz	192.9506	193.0494							L,H
E	193.3462	193.4938							L
1 Hz	193.9505	194.0495							L,H
1 Hz	194.9504	195.0496							L,H
1 Hz, 2 Hz	195.9503	196.0497							L,H
1 Hz	196.9502	197.0498							L,H
1 Hz	197.9501	198.0499							L,H
1 Hz	198.95	199.05							L,H
D	199.5106	199.6294							H
1 Hz	199.9499	200.0501							L,H
1 Hz	200.9498	201.0502							L,H
1 Hz	201.9497	202.0503							L,H

(Table continued)

TABLE IV. (*Continued*)

Line type	Mixed, isolated		Mixed, left		All fake data		Mixed, right		Detector
1 Hz	202.9496	203.0504							L,H
1 Hz, 2 Hz	203.9495	204.0505							L,H
1 Hz	204.9494	205.0506							L,H
1 Hz, 2 Hz	205.9493	206.0507							L,H
1 Hz	206.9492	207.0508							L,H
1 Hz	207.9491	208.0509							L,H
1 Hz	208.949	209.051							L,H
1 Hz	209.9489	210.0511							L,H
D	210.2995	210.4205							H
1 Hz	210.9488	211.0512							L,H
1 Hz	211.9487	212.0513							L,H
1 Hz	212.9486	213.0514							L,H
1 Hz, 2 Hz	213.9485	214.0515							L,H
1 Hz	214.9484	215.0516							L,H
1 Hz, 2 Hz	215.9483	216.0517							L,H
1 Hz	216.9482	217.0518							L,H
SB	217.491	217.5946							H
1 Hz, 2 Hz	217.9481	218.0519							L,H
1 Hz	218.948	219.052							L,H
1 Hz	219.9479	220.0521							L,H
1 Hz, 2 Hz	220.9478	221.0522							L,H
1 Hz, 2 Hz	221.9477	222.0523							L,H
1 Hz	222.9476	223.0524							L,H
1 Hz	223.9475	224.0525							L,H
1 Hz	224.9474	225.0526							L,H
1 Hz, 2 Hz	225.9473	226.0527							L,H
1 Hz	226.9472	227.0528							L,H
1 Hz	227.9471	228.0529							L,H
1 Hz	228.947	229.053							L,H
1 Hz	229.9469	230.0531							L,H
1 Hz	230.9468	231.0532							L,H
1 Hz	231.9467	232.0533							L,H
1 Hz	232.9466	233.0534							L,H
E	233.1272	233.3328							L
1 Hz, 2 Hz	233.9465	234.0535							L,H
1 Hz	234.9464	235.0536							L,H
1 Hz, 2 Hz	235.9463	236.0537							L,H
1 Hz	236.9462	237.0538							L,H
1 Hz	237.9461	238.0539							L,H
1 Hz, M			238.946	239.0528	239.0528	240.947	240.947	241.0542	L,H
E			241.6564	241.7636	241.7636	241.7964	241.7964	241.9036	L
1 Hz, 2 Hz	241.9457	242.0543							L,H
1 Hz	242.9456	243.0544							L,H
SB	243.1995	243.3083							H
1 Hz, 2 Hz	243.9455	244.0545							L,H
1 Hz	244.9454	245.0546							L,H
1 Hz	245.9453	246.0547							L,H
1 Hz	246.9452	247.0548							L,H
1 Hz, 2 Hz	247.9451	248.0549							L,H
1 Hz	248.945	249.055							L,H
1 Hz	249.9449	250.0551							L,H
1 Hz	250.9448	251.0552							L,H
1 Hz, 2 Hz	251.9447	252.0553							L,H
1 Hz	252.9446	253.0554							L,H
1 Hz, 2 Hz	253.9445	254.0555							L,H

(Table continued)

TABLE IV. (*Continued*)

Line type	Mixed, isolated		Mixed, left		All fake data		Mixed, right		Detector
1 Hz	254.9444	255.0556							L,H
1 Hz, 2 Hz	255.9443	256.0557							L,H
1 Hz	256.9442	257.0558							L,H
1 Hz	257.9441	258.0559							L,H
1 Hz	258.944	259.056							L,H
1 Hz, 2 Hz	259.9439	260.0561							L,H
1 Hz	260.9438	261.0562							L,H
1 Hz, 2 Hz	261.9437	262.0563							L,H
1 Hz	262.9436	263.0564							L,H
1 Hz, 2 Hz	263.9435	264.0565							L,H
1 Hz	264.9434	265.0566							L,H
1 Hz, 2 Hz	265.9433	266.0567							L,H
1 Hz	266.9432	267.0568							L,H
1 Hz, 2 Hz	267.9431	268.0569							L,H
SB	268.908	269.022							H
1 Hz	268.943	269.057							L,H
1 Hz, 2 Hz	269.9429	270.0571							L,H
1 Hz	270.9428	271.0572							L,H
1 Hz	271.9427	272.0573							L,H
1 Hz	272.9426	273.0574							L,H
1 Hz, 2 Hz	273.9425	274.0575							L,H
1 Hz	274.9424	275.0576							L,H
1 Hz	275.9423	276.0577							L,H
1 Hz	276.9422	277.0578							L,H
1 Hz, 2 Hz	277.9421	278.0579							L,H
1 Hz	278.942	279.058							L,H
1 Hz, 2 Hz	279.9419	280.0581							L,H
1 Hz	280.9418	281.0582							L,H
1 Hz, 2 Hz	281.9417	282.0583							L,H
1 Hz	282.9416	283.0584							L,H
1 Hz	283.9415	284.0585							L,H
1 Hz	284.9414	285.0586							L,H
1 Hz, 2 Hz	285.9413	286.0587							L,H
1 Hz	286.9412	287.0588							L,H
1 Hz	287.9411	288.0589							L,H
1 Hz	288.941	289.059							L,H
1 Hz, 2 Hz	289.9409	290.0591							L,H
1 Hz	290.9408	291.0592							L,H
1 Hz	291.9407	292.0593							L,H
1 Hz	292.9406	293.0594							L,H
1 Hz	293.9405	294.0595							L,H
SB	294.6161	294.7351							H
1 Hz	294.9404	295.0596							L,H
1 Hz	295.9403	296.0597							L,H
1 Hz	296.9402	297.0598							L,H
1 Hz, 2 Hz	297.9401	298.0599							L,H
1 Hz, M			298.94	299.0588	299.0588	300.941	300.941	301.0602	L,H
1 Hz	301.9397	302.0603							L,H
1 Hz	302.9396	303.0604							L,H
1 Hz	303.9395	304.0605							L,H
1 Hz	304.9394	305.0606							L,H
1 Hz	305.9393	306.0607							L,H
1 Hz	306.9392	307.0608							L,H
1 Hz, 2 Hz	307.9391	308.0609							L,H
1 Hz	308.939	309.061							L,H

(Table continued)

TABLE IV. (Continued)

Line type	Mixed, isolated		Mixed, left		All fake data		Mixed, right		Detector
1 Hz	309.9389	310.0611							L,H
1 Hz	310.9388	311.0612							L,H
1 Hz, 2 Hz	311.9387	312.0613							L,H
1 Hz	312.9386	313.0614							L,H
1 Hz	313.9385	314.0615							L,H
1 Hz	314.9384	315.0616							L,H
1 Hz, 2 Hz	315.9383	316.0617							L,H
1 Hz	316.9382	317.0618							L,H
1 Hz	317.9381	318.0619							L,H
1 Hz	318.938	319.062							L,H
1 Hz, 2 Hz	319.9379	320.0621							L,H
SB	320.3246	320.4488							H
1 Hz	320.9378	321.0622							L,H
1 Hz	321.9377	322.0623							L,H
1 Hz	322.9376	323.0624							L,H
1 Hz	323.9375	324.0625							L,H
1 Hz	324.9374	325.0626							L,H
1 Hz	325.9373	326.0627							L,H
1 Hz	326.9372	327.0628							L,H
1 Hz	327.9371	328.0629							L,H
1 Hz	328.937	329.063							L,H
VM			329.1476	329.2724	329.2724	329.3676	329.3676	329.4924	L
1 Hz, E, VM			329.3376	329.4624	329.4624	329.9381	329.9381	330.0631	H
1 Hz	329.9369	330.0631							L
1 Hz	330.9368	331.0632							L,H
1 Hz	331.9367	332.0633							L,H
1 Hz	332.9366	333.0634							L,H
1 Hz, 2 Hz	333.9365	334.0635							L,H
1 Hz	334.9364	335.0636							L,H
VM			335.187	335.313	335.313	335.747	335.747	335.873	L
1 Hz, VM			335.437	335.563	335.563	335.9375	335.9375	336.0637	H
1 Hz	335.9363	336.0637							L
1 Hz	336.9362	337.0638							L,H
1 Hz	337.9361	338.0639							L,H
1 Hz	338.936	339.064							L,H
1 Hz, VM			339.9359	340.0629	340.0629	349.9361	349.9361	350.0651	L
1 Hz	339.9359	340.0641							H
1 Hz	340.9358	341.0642							H
1 Hz, SB, VM			341.9357	342.0631	342.0631	349.9361	349.9361	350.0651	H
1 Hz	350.9348	351.0652							L,H
1 Hz	351.9347	352.0653							L,H
1 Hz	352.9346	353.0654							L,H
1 Hz	353.9345	354.0655							L,H
1 Hz	354.9344	355.0656							L,H
1 Hz	355.9343	356.0657							L,H
1 Hz	356.9342	357.0658							L,H
1 Hz	357.9341	358.0659							L,H
1 Hz, M			358.934	359.0648	359.0648	360.935	360.935	361.0662	L,H
1 Hz	361.9337	362.0663							L,H
1 Hz	362.9336	363.0664							L,H
1 Hz	363.9335	364.0665							L,H
1 Hz	364.9334	365.0666							L,H
1 Hz	365.9333	366.0667							L,H
1 Hz	366.9332	367.0668							L,H
1 Hz	367.9331	368.0669							L,H

(Table continued)

TABLE IV. (*Continued*)

Line type	Mixed, isolated		Mixed, left	All fake data	Mixed, right	Detector
1 Hz	368.933	369.067				L,H
1 Hz	369.9329	370.0671				L,H
1 Hz	370.9328	371.0672				L,H
SB	371.7405	371.8749				H
1 Hz, 2 Hz	371.9327	372.0673				L,H
1 Hz	372.9326	373.0674				L,H
D	373.3832	373.6168				H
1 Hz	373.9325	374.0675				L,H
1 Hz	374.9324	375.0676				L,H
1 Hz, 2 Hz	375.9323	376.0677				L,H
1 Hz	376.9322	377.0678				L,H
1 Hz	377.9321	378.0679				L,H
1 Hz	378.932	379.068				L,H
1 Hz, 2 Hz	379.9319	380.0681				L,H
1 Hz	380.9318	381.0682				L,H
1 Hz	381.9317	382.0683				L,H
1 Hz	382.9316	383.0684				L,H
SB	383.5955	383.7323				H
1 Hz, 2 Hz	383.9315	384.0685				L,H
1 Hz	384.9314	385.0686				L,H
1 Hz	385.9313	386.0687				L,H
1 Hz	386.9312	387.0688				L,H
1 Hz	387.9311	388.0689				L,H
1 Hz	388.931	389.069				L,H
1 Hz	389.9309	390.0691				L,H
1 Hz	390.9308	391.0692				L,H
1 Hz	391.9307	392.0693				L,H
D	392.1307	392.2693				L,H
1 Hz	392.9306	393.0694				L,H
1 Hz, 2 Hz	393.9305	394.0695				L,H
1 Hz	394.9304	395.0696				L,H
1 Hz	395.9303	396.0697				L,H
1 Hz	396.9302	397.0698				L,H
SB	397.4496	397.5892				H
1 Hz	397.9301	398.0699				L,H
1 Hz	398.93	399.07				L,H
D	399.23	399.37				L
1 Hz	399.9299	400.0701				L,H
1 Hz	400.9298	401.0702				L,H
D	401.3804	401.6196				H
1 Hz, 2 Hz	401.9297	402.0703				L,H
1 Hz	402.9296	403.0704				L,H
1 Hz	403.9295	404.0705				L,H
1 Hz	404.9294	405.0706				L,H
1 Hz	405.9293	406.0707				L,H
1 Hz	406.9292	407.0708				L,H
1 Hz	407.9291	408.0709				L,H
1 Hz	408.929	409.071				L,H
SB	409.2995	409.4415				H
1 Hz, 2 Hz	409.9289	410.0711				L,H
1 Hz	410.9288	411.0712				L,H
1 Hz	411.9287	412.0713				L,H
1 Hz	412.9286	413.0714				L,H
1 Hz, 2 Hz	413.9285	414.0715				L,H
1 Hz	414.9284	415.0716				L,H

(Table continued)

TABLE IV. (*Continued*)

Line type	Mixed, isolated		Mixed, left		All fake data		Mixed, right		Detector
1 Hz	415.9283	416.0717							L,H
1 Hz	416.9282	417.0718							L,H
1 Hz, 2 Hz	417.9281	418.0719							L,H
1 Hz, M			418.928	419.0708	419.0708	420.929	420.929	421.0722	L,H
1 Hz, 2 Hz	421.9277	422.0723							L,H
1 Hz	422.9276	423.0724							L,H
SB	423.1582	423.303							H
1 Hz	423.9275	424.0725							L,H
1 Hz	424.9274	425.0726							L,H
1 Hz	425.9273	426.0727							L,H
1 Hz	426.9272	427.0728							L,H
1 Hz	427.9271	428.0729							L,H
1 Hz	428.927	429.073							L,H
1 Hz, 2 Hz	429.9269	430.0731							L,H
1 Hz	430.9268	431.0732							L,H
1 Hz, 2 Hz	431.9267	432.0733							L,H
1 Hz	432.9266	433.0734							L,H
1 Hz	433.9265	434.0735							L,H
1 Hz, 2 Hz	434.9264	435.0736							L,H
SB	435.0125	435.1597							H
1 Hz	435.9263	436.0737							L,H
1 Hz	436.9262	437.0738							L,H
1 Hz	437.9261	438.0739							L,H
1 Hz	438.926	439.074							L,H
1 Hz, 2 Hz	439.9259	440.0741							L,H
1 Hz	440.9258	441.0742							L,H
1 Hz	441.9257	442.0743							L,H
1 Hz	442.9256	443.0744							L,H
1 Hz	443.9255	444.0745							L,H
1 Hz	444.9254	445.0746							L,H
1 Hz	445.9253	446.0747							L,H
1 Hz	446.9252	447.0748							L,H
1 Hz, 2 Hz	447.9251	448.0749							L,H
1 Hz	448.925	449.075							L,H
1 Hz	449.9249	450.0751							L,H
1 Hz	450.9248	451.0752							L,H
1 Hz	451.9247	452.0753							L,H
1 Hz	452.9246	453.0754							L,H
1 Hz	453.9245	454.0755							L,H
1 Hz	454.9244	455.0756							L,H
1 Hz	455.9243	456.0757							L,H
1 Hz	456.9242	457.0758							L,H
1 Hz	457.9241	458.0759							L,H
1 Hz	458.924	459.076							L,H
1 Hz	459.9239	460.0761							L,H
SB	460.7206	460.8728							H
1 Hz	460.9238	461.0762							L,H
1 Hz, 2 Hz	461.9237	462.0763							L,H
1 Hz	462.9236	463.0764							L,H
1 Hz	463.9235	464.0765							L,H
1 Hz	464.9234	465.0766							L,H
1 Hz, 2 Hz	465.9233	466.0767							L,H
1 Hz	466.9232	467.0768							L,H
1 Hz, 2 Hz	467.9231	468.0769							L,H
1 Hz	468.923	469.077							L,H

(Table continued)

TABLE IV. (*Continued*)

Line type	Mixed, isolated		Mixed, left		All fake data		Mixed, right		Detector
1 Hz, 2 Hz	469.9229	470.0771							L,H
1 Hz	470.9228	471.0772							L,H
1 Hz	471.9227	472.0773							L,H
1 Hz	472.9226	473.0774							L,H
1 Hz, 2 Hz	473.9225	474.0775							L,H
1 Hz	474.9224	475.0776							L,H
1 Hz	475.9223	476.0777							L,H
1 Hz	476.9222	477.0778							L,H
1 Hz	477.9221	478.0779							L,H
1 Hz, M			478.922	479.0768	479.0768	480.923	480.923	481.0782	L,H
1 Hz, 2 Hz	481.9217	482.0783							L,H
1 Hz	482.9216	483.0784							L,H
1 Hz	483.9215	484.0785							L,H
1 Hz	484.9214	485.0786							L,H
1 Hz	485.9213	486.0787							L,H
SB	486.4291	486.5865							H
1 Hz	486.9212	487.0788							L,H
1 Hz, 2 Hz	487.9211	488.0789							L,H
1 Hz	488.921	489.079							L,H
1 Hz	489.9209	490.0791							L,H
1 Hz	490.9208	491.0792							L,H
1 Hz	491.9207	492.0793							L,H
1 Hz	492.9206	493.0794							L,H
1 Hz	493.9205	494.0795							L,H
1 Hz	494.9204	495.0796							L,H
1 Hz, 2 Hz	495.9203	496.0797							L,H
1 Hz	496.9202	497.0798							L,H
1 Hz	497.9201	498.0799							L,H
1 Hz	498.92	499.08							L,H
1 Hz, 2 Hz	499.9199	500.0801							L,H
1 Hz	500.9198	501.0802							L,H
1 Hz	501.9197	502.0803							L,H
1 Hz	502.9196	503.0804							L,H
1 Hz, 2 Hz	503.9195	504.0805							L,H
1 Hz	504.9194	505.0806							L,H
1 Hz	505.9193	506.0807							L,H
1 Hz	506.9192	507.0808							L,H
1 Hz, 2 Hz	507.9191	508.0809							L,H
1 Hz	508.919	509.081							L,H

4. Signal-frequency ranges where the results might have contributions from fake data

TABLE V. 50-mHz search-frequency bands that were identified as disturbed based on visual inspection (D) or where the results were produced from entirely fake data as detailed in Table I (C). Both sets of bands (D and C) were excluded from the analysis. The first two columns list the first frequency of the first and last 50-mHz band in a contiguous range of excluded bands.

Start band	Stop band	Disturbance type
50.113		D
50.563		D
51.013		D
51.113	51.163	D
51.963		D
52.413	52.463	D
52.613		D
52.863	53.113	D
53.663		D
53.863	53.913	D
54.363	54.513	D
55.063	55.113	D
55.463	55.613	D
55.713	55.963	D
56.113	56.513	D
56.613		D
57.563		D
58.163		D
58.363	58.613	D
58.713	59.013	D
59.063		C
59.113		C D
59.163	60.863	C
60.913		C D
60.963	61.013	D
61.313	61.613	D
61.963		D
62.213	62.263	D
62.363		D
63.163	63.213	D
63.463	63.513	D
63.713		D
64.013	64.113	D
64.313	64.513	D
64.713	64.813	D
65.313	65.413	D
68.513		D
68.763	68.913	D
69.263		D
69.713	69.763	D
70.063	70.113	D
70.463	70.513	D
71.063		D
71.513		D
72.013	72.113	D
72.313	72.413	D
72.913	73.013	D

(Table continued)

TABLE V. (Continued)

Start band	Stop band	Disturbance type
73.313	73.413	D
73.763	73.863	D
74.463	74.513	D
74.713		D
75.763		D
76.013	76.113	D
77.563	77.663	D
78.213	78.313	D
78.413	78.563	D
78.963	79.013	D
79.263		D
79.913	80.063	D
80.413	80.463	D
80.563	80.663	D
80.913		D
81.013	81.213	D
83.463		D
83.863		D
85.413		D
85.563		D
85.713	85.813	D
85.963		D
86.513		D
86.713	86.813	D
87.763		D
88.513		D
88.963		D
89.963	90.013	D
90.563	90.713	D
91.513		D
92.113		D
93.063	93.113	D
93.913	94.013	D
94.213		D
96.663	97.163	D
98.263		D
98.863	99.063	D
99.713	99.763	D
99.863	100.013	D
100.213	100.263	D
100.463		D
102.163	102.263	D
102.663		D
103.013	103.113	D
103.413	103.463	D
104.863		D
105.663	105.713	D
106.413	106.663	D
107.013	107.213	D
107.313	107.413	D
107.663		D
108.013	108.063	D
108.813	109.113	D
109.413	109.513	D
109.963		D

(Table continued)

TABLE V. (*Continued*)

Start band	Stop band	Disturbance type
110.613		D
110.863	110.913	D
111.013	111.113	D
111.713	111.863	D
112.663	112.713	D
113.063		D
113.213	113.313	D
113.713	113.913	D
114.663	114.713	D
115.313	115.413	D
115.763		D
117.463	117.713	D
118.063		D
118.213	118.563	D
118.813	119.013	D
119.063	120.863	C
120.963	121.013	D
121.163	121.313	D
121.613	121.763	D
122.063	122.313	D
123.113		D
125.613	125.663	D
126.213	126.313	D
126.413		D
126.713	126.813	D
127.063		D
127.963	128.013	D
128.363		D
129.713	129.763	D
129.863	129.963	D
130.513		D
131.263		D
132.713	132.763	D
133.413		D
134.013	134.063	D
134.413	134.513	D
135.063	135.163	D
135.613	135.713	D
137.063	137.113	D
137.463	137.513	D
137.613	137.913	D
138.163		D
139.463	139.513	D
139.613	139.813	D
140.113	140.213	D
140.363	140.413	D
140.963		D
141.613	141.663	D
141.813	141.863	D
142.213	142.313	D
142.613	142.713	D
144.313	144.363	D
144.613	144.763	D
145.013	145.713	D
146.313	146.363	D

(Table continued)

TABLE V. (*Continued*)

Start band	Stop band	Disturbance type
146.663	146.813	D
146.913		D
147.113	147.163	D
147.713		D
148.763		D
149.113	149.213	D
149.563		D
149.963	150.013	D
150.863		D
151.263		D
152.063		D
153.163	153.313	D
153.413		D
153.613	153.713	D
153.863	153.913	D
154.213	154.263	D
155.263		D
155.763		D
156.113		D
156.213	156.263	D
156.363		D
156.513		D
156.813	156.863	D
157.363	157.413	D
157.763		D
158.163		D
158.363		D
160.213	160.313	D
161.413	161.513	D
162.313	162.363	D
162.913	162.963	D
163.463	163.513	D
168.063	168.113	D
169.613	169.713	D
170.813		D
173.713	173.813	D
174.163		D
178.513		D
178.963		D
179.063	180.863	C
180.963	181.013	D
181.363		D
181.813	181.863	D
182.763	182.813	D
184.363	184.463	D
185.363	185.413	D
187.963		D
188.463		D
189.363	189.413	D
189.813	189.863	D
190.763	190.813	D
192.363	192.613	D
193.613	194.313	D
196.963	197.013	D
197.713	197.763	D

(Table continued)

TABLE V. (*Continued*)

Start band	Stop band	Disturbance type
197.863	197.963	D
198.113	198.163	D
198.563	198.663	D
199.213	199.313	D
199.513	199.613	D
199.813	200.013	D
200.413	200.513	D
200.913	201.013	D
201.313	201.363	D
203.663		D
204.113	204.213	D
204.863	204.913	D
205.663		D
205.863		D
206.413	206.663	D
209.213	209.263	D
210.213	210.313	D
215.513		D
217.463	217.563	D
217.913	218.013	D
223.563	223.613	D
225.513	225.563	D
229.363		D
229.813	229.913	D
230.213	230.313	D
231.313	231.413	D
234.113	234.163	D
239.063	240.863	C
241.613	241.713	D
241.813	241.863	D
242.113	242.163	D
242.313	242.863	D
246.513	246.563	D
249.963	250.013	D
253.063	253.113	D
255.063	255.113	D
257.063	257.113	D
257.263	257.363	D
259.063	259.113	D
270.163	270.213	D
270.613	270.663	D
272.413	272.513	D
275.213	275.563	D
279.763	279.813	D
280.313	280.363	D
280.813		D
281.913	282.013	D
289.363		D
290.963	291.013	D
291.213		D
291.313	291.413	D
299.063	300.863	C
306.463	306.563	D
308.463	308.513	D
324.013	324.063	D

*(Table continued)*TABLE V. (*Continued*)

Start band	Stop band	Disturbance type
329.113	329.263	D
329.313		C
329.463	329.863	C
332.163	332.263	D
335.163	335.263	D
335.313	335.663	C
335.713		C D
335.763		C D
335.813		C D
335.863		C
338.613	338.863	D
339.013	339.213	D
339.463	340.013	D
340.063		C D
340.113	349.863	C
349.963	350.563	D
350.663	350.763	D
350.913	351.213	D
351.363	351.563	D
357.863	357.963	D
358.913	359.063	D
359.113	360.863	C
360.913	361.013	D
365.563	365.613	D
366.513	366.613	D
366.863		D
369.763	369.813	D
370.013	370.163	D
373.263	373.313	D
373.513	373.613	D
374.163		D
374.513	374.613	D
389.513	389.613	D
391.213	391.313	D
392.063	392.213	D
392.513	392.613	D
393.013	393.263	D
393.413	393.513	D
393.913		D
394.013	394.213	D
394.813	394.913	D
395.463	395.513	D
395.863		D
395.963	396.063	D
396.513	396.713	D
399.063	399.113	D
399.213	399.313	D
399.613	400.613	D
400.713	400.813	D
401.013	401.313	D
403.513	403.913	D
407.213	407.363	D
407.813	407.913	D
408.213	408.363	D
409.263	409.413	D

(Table continued)

TABLE V. (*Continued*)

Start band	Stop band	Disturbance type
413.013	413.363	D
416.113	416.213	D
417.013	417.213	D
418.163	418.213	D
419.113	420.863	C
421.213		D

*(Table continued)*TABLE V. (*Continued*)

Start band	Stop band	Disturbance type
430.313		D
444.413	444.513	D
448.913		D
451.413	451.663	D
472.563	472.663	D
474.563	474.613	D
479.113	480.863	C

- [1] <https://www.einsteinathome.org/>.
- [2] B. P. Abbott *et al.* (LIGO Scientific and Virgo Collaborations), Comprehensive all-sky search for periodic gravitational waves in the sixth science run LIGO data, *Phys. Rev. D* **94**, 042002 (2016).
- [3] A. Singh, M. A. Papa, H.-B. Eggenstein, S. Zhu, H. Pletsch, B. Allen, O. Bock, B. Maschenchalk, R. Prix, and X. Siemens, Results of an all-sky high-frequency Einstein@Home search for continuous gravitational waves in LIGO fifth science run, *Phys. Rev. D* **94**, 064061 (2016).
- [4] J. Aasi *et al.* (LIGO Scientific and Virgo Collaborations), First low frequency all-sky search for continuous gravitational wave signals, *Phys. Rev. D* **93**, 042007 (2016).
- [5] B. P. Abbott *et al.* (LIGO Scientific Collaboration), Einstein@Home all-sky search for periodic gravitational waves in LIGO S5 data, *Phys. Rev. D* **87**, 042001 (2013).
- [6] J. Abadie *et al.* (LIGO Scientific and Virgo Collaborations), All-sky search for periodic gravitational waves in the full S5 data, *Phys. Rev. D* **85**, 022001 (2012).
- [7] B. P. Abbott *et al.* (LIGO Scientific Collaboration), Einstein@Home search for periodic gravitational waves in early S5 LIGO data, *Phys. Rev. D* **80**, 042003 (2009).
- [8] B. P. Abbott *et al.* (LIGO Scientific Collaboration), All-sky LIGO search for periodic gravitational waves in the early S5 data, *Phys. Rev. Lett.* **102**, 111102 (2009).
- [9] B. Abbott *et al.* (LIGO Scientific Collaboration), All-sky search for periodic gravitational waves in LIGO S4 data, *Phys. Rev. D* **77**, 022001 (2008).
- [10] B. Abbott *et al.* (LIGO Scientific Collaboration), Einstein@Home search for periodic gravitational waves in LIGO S4 data, *Phys. Rev. D* **79**, 022001 (2009).
- [11] B. Abbott *et al.* (LIGO Scientific Collaboration), Searches for periodic gravitational waves from unknown isolated sources and Scorpius X-1: Results from the second LIGO science run, *Phys. Rev. D* **76**, 082001 (2007).
- [12] B. P. Abbott *et al.* (LIGO Scientific Collaboration), LIGO: The laser interferometer gravitational-wave observatory, *Rep. Prog. Phys.* **72**, 076901 (2009).
- [13] J. Abadie *et al.* (LIGO Scientific and Virgo Collaborations), Sensitivity achieved by the LIGO and Virgo gravitational wave detectors during LIGO's sixth and Virgo's second and third science runs, [arXiv:1203.2674](https://arxiv.org/abs/1203.2674).
- [14] J. Aasi *et al.* (LIGO Scientific Collaboration), Advanced LIGO, *Classical Quantum Gravity* **32**, 074001 (2015).
- [15] M. Shaltev, Optimizing the StackSlide setup and data selection for continuous-gravitational-wave searches in realistic detector data, *Phys. Rev. D* **93**, 044058, 2016.
- [16] J. Aasi *et al.* (LIGO Scientific and Virgo Collaborations), Characterization of the LIGO detectors during their sixth science run, *Classical Quantum Gravity* **32**, 115012 (2015).
- [17] H. J. Pletsch, Parameter-space correlations of the optimal statistic for continuous gravitational-wave detection, *Phys. Rev. D* **78**, 102005 (2008).
- [18] H. J. Pletsch, Parameter-space metric of semicoherent searches for continuous gravitational waves, *Phys. Rev. D* **82**, 042002 (2010).
- [19] C. Cutler and B. F. Schutz, The generalized \mathcal{F} -statistic: multiple detectors and multiple gravitational wave pulsars, *Phys. Rev. D* **72**, 063006 (2005).
- [20] J. Aasi *et al.* (LIGO Scientific and Virgo Collaborations), Directed search for continuous gravitational waves from the Galactic Center, *Phys. Rev. D* **88**, 102002 (2013).
- [21] D. Keitel, R. Prix, M. A. Papa, P. Leaci, and M. Siddiqi, Search for continuous gravitational waves: Improving robustness versus instrumental artifacts, *Phys. Rev. D* **89**, 064023 (2014).
- [22] B. Behnke, M. A. Papa, and R. Prix, Postprocessing methods used in the search for continuous gravitational-wave signals from the Galactic Center, *Phys. Rev. D* **91**, 064007 (2015).
- [23] Karl Wette, Estimating the sensitivity of wide-parameter-space searches for gravitational-wave pulsars, *Phys. Rev. D* **85**, 042003 (2012).
- [24] J. Ming, B. Krishnan, M. A. Papa, C. Aulbert, and H. Fehrmann, Optimal directed searches for continuous gravitational waves, *Phys. Rev. D* **93**, 064011 (2016).

B. P. Abbott,¹ R. Abbott,¹ T. D. Abbott,² M. R. Abernathy,³ F. Acernese,^{4,5} K. Ackley,⁶ C. Adams,⁷ T. Adams,⁸ P. Addesso,⁹ R. X. Adhikari,¹ V. B. Adya,¹⁰ C. Affeldt,¹⁰ M. Agathos,¹¹ K. Agatsuma,¹¹ N. Aggarwal,¹² O. D. Aguiar,¹³ L. Aiello,^{14,15} A. Ain,¹⁶ B. Allen,^{10,18,19} A. Allocca,^{20,21} P. A. Altin,²² S. B. Anderson,¹ W. G. Anderson,¹⁸ K. Arai,¹ M. C. Araya,¹ C. C. Arceneaux,²³ J. S. Areeda,²⁴ N. Arnaud,²⁵ K. G. Arun,²⁶ S. Ascenzi,^{27,15} G. Ashton,²⁸ M. Ast,²⁹ S. M. Aston,⁷ P. Astone,³⁰ P. Aufmuth,¹⁹ C. Aulbert,¹⁰ S. Babak,³¹ P. Bacon,³² M. K. M. Bader,¹¹ P. T. Baker,³³ F. Baldaccini,^{34,35} G. Ballardín,³⁶ S. W. Ballmer,³⁷ J. C. Barayoga,¹ S. E. Barclay,³⁸ B. C. Barish,¹ D. Barker,³⁹ F. Barone,^{4,5} B. Barr,³⁸ L. Barsotti,¹² M. Barsuglia,³² D. Barta,⁴⁰ J. Bartlett,³⁹ I. Bartos,⁴¹ R. Bassiri,⁴² A. Basti,^{20,21} J. C. Batch,³⁹ C. Baune,¹⁰ V. Vavivadda,³⁶ M. Bazzan,^{43,44} M. Bejger,⁴⁵ A. S. Bell,³⁸ B. K. Berger,¹ G. Bergmann,¹⁰ C. P. L. Berry,⁴⁶ D. Bersanetti,^{47,48} A. Bertolini,¹¹ J. Betzwieser,⁷ S. Bhagwat,³⁷ R. Bhandare,⁴⁹ I. A. Bilenko,⁵⁰ G. Billingsley,¹ J. Birch,⁷ R. Birney,⁵¹ S. Biscans,¹² A. Bisht,^{10,19} M. Bitossi,³⁶ C. Biwer,³⁷ M. A. Bizouard,²⁵ J. K. Blackburn,¹ C. D. Blair,⁵² D. G. Blair,⁵² R. M. Blair,³⁹ S. Bloemen,⁵³ O. Bock,¹⁰ M. Boer,⁵⁴ G. Bogaert,⁵⁴ C. Bogan,¹⁰ A. Bohe,³¹ C. Bond,⁴⁶ F. Bondu,⁵⁵ R. Bonnand,⁸ B. A. Boom,¹¹ R. Bork,¹ V. Boschi,^{20,21} S. Bose,^{56,16} Y. Bouffanais,³² A. Bozzi,³⁶ C. Bradaschia,²¹ P. R. Brady,¹⁸ V. B. Braginsky,^{50,†} M. Branchesi,^{57,58} J. E. Brau,⁵⁹ T. Briant,⁶⁰ A. Brillet,⁵⁴ M. Brinkmann,¹⁰ V. Brisson,²⁵ P. Brockill,¹⁸ J. E. Broida,⁶¹ A. F. Brooks,¹ D. A. Brown,³⁷ D. D. Brown,⁴⁶ N. M. Brown,¹² S. Brunett,¹ C. C. Buchanan,² A. Buikema,¹² T. Bulik,⁶² H. J. Bulten,^{63,11} A. Buonanno,^{31,64} D. Buskulic,⁸ C. Buy,³² R. L. Byer,⁴² M. Cabero,¹⁰ L. Cadonati,⁶⁵ G. Cagnoli,^{66,67} C. Cahillane,¹ J. Calderón Bustillo,⁶⁵ T. Callister,¹ E. Calloni,^{68,5} J. B. Camp,⁶⁹ K. C. Cannon,⁷⁰ J. Cao,⁷¹ C. D. Capano,¹⁰ E. Capocasa,³² F. Carbognani,³⁶ S. Caride,⁷² J. Casanueva Diaz,²⁵ C. Casentini,^{27,15} S. Caudill,¹⁸ M. Cavaglià,²³ F. Cavalier,²⁵ R. Cavalieri,³⁶ G. Cella,²¹ C. B. Cepeda,¹ L. Cerboni Baiardi,^{57,58} G. Cerretani,^{20,21} E. Cesarini,^{27,15} S. J. Chamberlin,⁷³ M. Chan,³⁸ S. Chao,⁷⁴ P. Charlton,⁷⁵ E. Chassande-Mottin,³² B. D. Cheeseboro,⁷⁶ H. Y. Chen,⁷⁷ Y. Chen,⁷⁸ C. Cheng,⁷⁴ A. Chincarini,⁴⁸ A. Chiummo,³⁶ H. S. Cho,⁷⁹ M. Cho,⁶⁴ J. H. Chow,²² N. Christensen,⁶¹ Q. Chu,⁵² S. Chua,⁶⁰ S. Chung,⁵² G. Ciani,⁶ F. Clara,³⁹ J. A. Clark,⁶⁵ F. Cleva,⁵⁴ E. Coccia,^{27,14} P.-F. Cohadon,⁶⁰ A. Colla,^{80,30} C. G. Collette,⁸¹ L. Cominsky,⁸² M. Constancio Jr.,¹³ A. Conte,^{80,30} L. Conti,⁴⁴ D. Cook,³⁹ T. R. Corbitt,² N. Cornish,³³ A. Corsi,⁷² S. Cortese,³⁶ C. A. Costa,¹³ M. W. Coughlin,⁶¹ S. B. Coughlin,⁸³ J.-P. Coulon,⁵⁴ S. T. Countryman,⁴¹ P. Couvares,¹ E. E. Cowan,⁶⁵ D. M. Coward,⁵² M. J. Cowart,⁷ D. C. Coyne,¹ R. Coyne,⁷² K. Craig,³⁸ J. D. E. Creighton,¹⁸ T. D. Creighton,⁸⁸ J. Cripe,² S. G. Crowder,⁸⁴ A. Cumming,³⁸ L. Cunningham,³⁸ E. Cuoco,³⁶ T. Dal Canton,¹⁰ S. L. Danilishin,³⁸ S. D'Antonio,¹⁵ K. Danzmann,^{19,10} N. S. Darman,⁸⁵ A. Dasgupta,⁸⁶ C. F. Da Silva Costa,⁶ V. Dattilo,³⁶ I. Dave,⁴⁹ M. Davier,²⁵ G. S. Davies,³⁸ E. J. Daw,⁸⁷ R. Day,³⁶ S. De,³⁷ D. DeBra,⁴² G. Debreczeni,⁴⁰ J. Degallaix,⁶⁶ M. De Laurentis,^{68,5} S. Deléglise,⁶⁰ W. Del Pozzo,⁴⁶ T. Denker,¹⁰ T. Dent,¹⁰ V. Dergachev,¹ R. De Rosa,^{68,5} R. T. DeRosa,⁷ R. DeSalvo,⁹ R. C. Devine,⁷⁶ S. Dhurandhar,¹⁶ M. C. Díaz,⁸⁸ L. Di Fiore,⁵ M. Di Giovanni,^{89,90} T. Di Girolamo,^{68,5} A. Di Lieto,^{20,21} S. Di Pace,^{80,30} I. Di Palma,^{31,80,30} A. Di Virgilio,²¹ V. Dolique,⁶⁶ F. Donovan,¹² K. L. Dooley,²³ S. Doravari,¹⁰ R. Douglas,³⁸ T. P. Downes,¹⁸ M. Drago,¹⁰ R. W. P. Drever,¹ J. C. Driggers,³⁹ M. Ducret,⁸ S. E. Dwyer,³⁹ T. B. Edo,⁸⁷ M. C. Edwards,⁶¹ A. Effler,⁷ H.-B. Eggenstein,¹⁰ P. Ehrens,¹ J. Eichholz,^{6,1} S. S. Eikenberry,⁶ W. Engels,⁷⁸ R. C. Essick,¹² T. Etzel,¹ M. Evans,¹² T. M. Evans,⁷ R. Everett,⁷³ M. Factourovich,⁴¹ V. Fafone,^{27,15} H. Fair,³⁷ S. Fairhurst,⁹¹ X. Fan,⁷¹ Q. Fang,⁵² S. Farinon,⁴⁸ B. Farr,⁷⁷ W. M. Farr,⁴⁶ M. Favata,⁹² M. Fays,⁹¹ H. Fehrmann,¹⁰ M. M. Fejer,⁴² E. Fenyvesi,⁹³ I. Ferrante,^{20,21} E. C. Ferreira,¹³ F. Ferrini,³⁶ F. Fidecaro,^{20,21} I. Fiori,³⁶ D. Fiorucci,³² R. P. Fisher,³⁷ R. Flaminio,^{66,94} M. Fletcher,³⁸ J.-D. Fournier,⁵⁴ S. Frasca,^{80,30} F. Frasconi,²¹ Z. Frei,⁹³ A. Freise,⁴⁶ R. Frey,⁵⁹ V. Frey,²⁵ P. Fritschel,¹² V. V. Frolov,⁷ P. Fulda,⁶ M. Fyffe,⁷ H. A. G. Gabbard,²³ J. R. Gair,⁹⁵ L. Gammaitoni,³⁴ S. G. Gaonkar,¹⁶ F. Garufi,^{68,5} G. Gaur,^{96,86} N. Gehrels,⁶⁹ G. Gemme,⁴⁸ P. Geng,⁸⁸ E. Genin,³⁶ A. Gennai,²¹ J. George,⁴⁹ L. Gergely,⁹⁷ V. Germain,⁸ Abhirup Ghosh,¹⁷ Archisman Ghosh,¹⁷ S. Ghosh,^{53,11} J. A. Giaime,^{2,7} K. D. Giardino,⁷ A. Giazotto,²¹ K. Gill,⁹⁸ A. Glaefke,³⁸ E. Goetz,³⁹ R. Goetz,⁶ L. Gondan,⁹³ G. González,² J. M. Gonzalez Castro,^{20,21} A. Gopakumar,⁹⁹ N. A. Gordon,³⁸ M. L. Gorodetsky,⁵⁰ S. E. Gossan,¹ M. Gosselin,³⁶ R. Gouaty,⁸ A. Grado,^{100,5} C. Graef,³⁸ P. B. Graff,⁶⁴ M. Granata,⁶⁶ A. Grant,³⁸ S. Gras,¹² C. Gray,³⁹ G. Greco,^{57,58} A. C. Green,⁴⁶ P. Groot,⁵³ H. Grote,¹⁰ S. Grunewald,³¹ G. M. Guidi,^{57,58} X. Guo,⁷¹ A. Gupta,¹⁶ M. K. Gupta,⁸⁶ K. E. Gushwa,¹ E. K. Gustafson,¹ R. Gustafson,¹⁰¹ J. J. Hacker,²⁴ B. R. Hall,⁵⁶ E. D. Hall,¹ G. Hammond,³⁸ M. Haney,⁹⁹ M. M. Hanke,¹⁰ J. Hanks,³⁹ C. Hanna,⁷³ J. Hanson,⁷ T. Hardwick,² J. Harms,^{57,58} G. M. Harry,³ I. W. Harry,³¹ M. J. Hart,³⁸ M. T. Hartman,⁶ C.-J. Haster,⁴⁶ K. Haughian,³⁸ A. Heidmann,⁶⁰ M. C. Heintze,⁷ H. Heitmann,⁵⁴ P. Hello,²⁵ G. Hemming,³⁶ M. Hendry,³⁸ I. S. Heng,³⁸ J. Hennig,³⁸ J. Henry,¹⁰² A. W. Heptonstall,¹ M. Heurs,^{10,19} S. Hild,³⁸ D. Hoak,³⁶ D. Hofman,⁶⁶ K. Holt,⁷ D. E. Holz,⁷⁷ P. Hopkins,⁹¹ J. Hough,³⁸ E. A. Houston,³⁸ E. J. Howell,⁵² Y. M. Hu,¹⁰ S. Huang,⁷⁴ E. A. Huerta,¹⁰³ D. Huet,²⁵ B. Hughey,⁹⁸ S. Husa,¹⁰⁴ S. H. Huttner,³⁸ T. Huynh-Dinh,⁷ N. Indik,¹⁰ D. R. Ingram,³⁹ R. Inta,⁷² H. N. Isa,³⁸ J.-M. Isac,⁶⁰

M. Isi,¹ T. Isogai,¹² B. R. Iyer,¹⁷ K. Izumi,³⁹ T. Jacqmin,⁶⁰ H. Jang,⁷⁹ K. Jani,⁶⁵ P. Jaranowski,¹⁰⁵ S. Jawahar,¹⁰⁶ L. Jian,⁵² F. Jiménez-Forteza,¹⁰⁴ W. W. Johnson,² D. I. Jones,²⁸ R. Jones,³⁸ R. J. G. Jonker,¹¹ L. Ju,⁵² Haris K,¹⁰⁷ C. V. Kalaghatgi,⁹¹ V. Kalogera,⁸³ S. Kandhasamy,²³ G. Kang,⁷⁹ J. B. Kanner,¹ S. J. Kapadia,¹⁰ S. Karki,⁵⁹ K. S. Karvinen,¹⁰ M. Kasprzack,^{36,2} E. Katsavounidis,¹² W. Katzman,⁷ S. Kaufer,¹⁹ T. Kaur,⁵² K. Kawabe,³⁹ F. Kéfélian,⁵⁴ M. S. Kehl,¹⁰⁸ D. Keitel,¹⁰⁴ D. B. Kelley,³⁷ W. Kells,¹ R. Kennedy,⁸⁷ J. S. Key,⁸⁸ F. Y. Khalili,⁵⁰ I. Khan,¹⁴ S. Khan,⁹¹ Z. Khan,⁸⁶ E. A. Khazanov,¹⁰⁹ N. Kijbunchoo,³⁹ Chi-Woong Kim,⁷⁹ Chunglee Kim,⁷⁹ J. Kim,¹¹⁰ K. Kim,¹¹¹ N. Kim,⁴² W. Kim,¹¹² Y.-M. Kim,¹¹⁰ S. J. Kimbrell,⁶⁵ E. J. King,¹¹² P. J. King,³⁹ J. S. Kissel,³⁹ B. Klein,⁸³ L. Kleybolte,²⁹ S. Klimenko,⁶ S. M. Koehlenbeck,¹⁰ S. Koley,¹¹ V. Kondrashov,¹ A. Kontos,¹² M. Korobko,²⁹ W. Z. Korth,¹ I. Kowalska,⁶² D. B. Kozak,¹ V. Kringel,¹⁰ B. Krishnan,¹⁰ A. Królak,^{113,114} C. Krueger,¹⁹ G. Kuehn,¹⁰ P. Kumar,¹⁰⁸ R. Kumar,⁸⁶ L. Kuo,⁷⁴ A. Kutynia,¹¹³ B. D. Lackey,³⁷ M. Landry,³⁹ J. Lange,¹⁰² B. Lantz,⁴² P. D. Lasky,¹¹⁵ M. Laxen,⁷ C. Lazzaro,⁴⁴ P. Leaci,^{80,30} S. Leavey,³⁸ E. O. Lebigot,^{32,71} C. H. Lee,¹¹⁰ H. K. Lee,¹¹¹ H. M. Lee,¹¹⁶ K. Lee,³⁸ A. Lenon,³⁷ M. Leonardi,^{89,90} J. R. Leong,¹⁰ N. Leroy,²⁵ N. Letendre,⁸ Y. Levin,¹¹⁵ J. B. Lewis,¹ T. G. F. Li,¹¹⁷ A. Libson,¹² T. B. Littenberg,¹¹⁸ N. A. Lockerbie,¹⁰⁶ A. L. Lombardi,¹¹⁹ L. T. London,⁹¹ J. E. Lord,³⁷ M. Lorenzini,^{14,15} V. Loriette,¹²⁰ M. Lormand,⁷ G. Losurdo,⁵⁸ J. D. Lough,^{10,19} H. Lück,^{19,10} A. P. Lundgren,¹⁰ R. Lynch,¹² Y. Ma,⁵² B. Machenschalk,¹⁰ M. MacInnis,¹² D. M. Macleod,² F. Magaña-Sandoval,³⁷ L. Magaña Zertuche,³⁷ R. M. Magee,⁵⁶ E. Majorana,³⁰ I. Maksimovic,¹²⁰ V. Malvezzi,^{27,15} N. Man,⁵⁴ V. Mandic,⁸⁴ V. Mangano,³⁸ G. L. Mansell,²² M. Manske,¹⁸ M. Mantovani,³⁶ F. Marchesoni,^{121,35} F. Marion,⁸ S. Márka,⁴¹ Z. Márka,⁴¹ A. S. Markosyan,⁴² E. Maros,¹ F. Martelli,^{57,58} L. Martellini,⁵⁴ I. W. Martin,³⁸ D. V. Martynov,¹² J. N. Marx,¹ K. Mason,¹² A. Masserot,⁸ T. J. Massinger,³⁷ M. Masso-Reid,³⁸ S. Mastrogiovanni,^{80,30} F. Matichard,¹² L. Matone,⁴¹ N. Mavalvala,¹² N. Mazumder,⁵⁶ R. McCarthy,³⁹ D. E. McClelland,²² S. McCormick,⁷ S. C. McGuire,¹²² G. McIntyre,¹ J. McIver,¹ D. J. McManus,²² T. McRae,²² S. T. McWilliams,⁷⁶ D. Meacher,⁷³ G. D. Meadors,^{31,10} J. Meidam,¹¹ A. Melatos,⁸⁵ G. Mendell,³⁹ R. A. Mercer,¹⁸ E. L. Merilh,³⁹ M. Merzougui,⁵⁴ S. Meshkov,¹ C. Messenger,³⁸ C. Messick,⁷³ R. Metzdrorf,⁶⁰ P. M. Meyers,⁸⁴ F. Mezzani,^{30,80} H. Miao,⁴⁶ C. Michel,⁶⁶ H. Middleton,⁴⁶ E. E. Mikhailov,¹²³ L. Milano,^{68,5} A. L. Miller,^{6,80,30} A. Miller,⁸³ B. B. Miller,⁸³ J. Miller,¹² M. Millhouse,³³ Y. Minenkov,¹⁵ J. Ming,³¹ S. Mirshekari,¹²⁴ C. Mishra,¹⁷ S. Mitra,¹⁶ V. P. Mitrofanov,⁵⁰ G. Mitselmakher,⁶ R. Mittleman,¹² A. Moggi,²¹ M. Mohan,³⁶ S. R. P. Mohapatra,¹² M. Montani,^{57,58} B. C. Moore,⁹² C. J. Moore,¹²⁵ D. Moraru,³⁹ G. Moreno,³⁹ S. R. Morris,⁸⁸ K. Mossavi,¹⁰ B. Mours,⁸ C. M. Mow-Lowry,⁴⁶ G. Mueller,⁶ A. W. Muir,⁹¹ Arunava Mukherjee,¹⁷ D. Mukherjee,¹⁸ S. Mukherjee,⁸⁸ N. Mukund,¹⁶ A. Mullavey,⁷ J. Munch,¹¹² D. J. Murphy,⁴¹ P. G. Murray,³⁸ A. Mytidis,⁶ I. Nardecchia,^{27,15} L. Naticchioni,^{80,30} R. K. Nayak,¹²⁶ K. Nedkova,¹¹⁹ G. Nelemans,^{53,11} T. J. N. Nelson,⁷ M. Neri,^{47,48} A. Neunzert,¹⁰¹ G. Newton,³⁸ T. T. Nguyen,²² A. B. Nielsen,¹⁰ S. Nissanke,^{53,11} A. Nitz,¹⁰ F. Nocera,³⁶ D. Nolting,⁷ M. E. N. Normandin,⁸⁸ L. K. Nuttall,³⁷ J. Oberling,³⁹ E. Ochsner,¹⁸ J. O'Dell,¹²⁷ E. Oelker,¹² G. H. Ogil,¹²⁸ J. J. Oh,¹²⁹ S. H. Oh,¹²⁹ F. Ohme,⁹¹ M. Oliver,¹⁰⁴ P. Oppermann,¹⁰ Richard J. Oram,⁷ B. O'Reilly,⁷ R. O'Shaughnessy,¹⁰² D. J. Ottaway,¹¹² H. Overmier,⁷ B. J. Owen,⁷² A. Pai,¹⁰⁷ S. A. Pai,⁴⁹ J. R. Palamos,⁵⁹ O. Palashov,¹⁰⁹ C. Palomba,³⁰ A. Pal-Singh,²⁹ H. Pan,⁷⁴ C. Pankow,⁸³ F. Pannarale,⁹¹ B. C. Pant,⁴⁹ F. Paoletti,^{36,21} A. Paoli,³⁶ M. A. Papa,^{31,18,10} H. R. Paris,⁴² W. Parker,⁷ D. Pascucci,³⁸ A. Pasqualetti,³⁶ R. Passaquieti,^{20,21} D. Passuello,²¹ B. Patricelli,^{20,21} Z. Patrick,⁴² B. L. Pearlstone,³⁸ M. Pedraza,¹ R. Pedurand,^{66,130} L. Pekowsky,³⁷ A. Pele,⁷ S. Penn,¹³¹ A. Perreca,¹ L. M. Perri,⁸³ M. Phelps,³⁸ O. J. Piccinni,^{80,30} M. Pichot,⁵⁴ F. Piergiovanni,^{57,58} V. Pierro,⁹ G. Pillant,³⁶ L. Pinard,⁶⁶ I. M. Pinto,⁹ M. Pitkin,³⁸ M. Poe,¹⁸ R. Poggiani,^{20,21} P. Popolizio,³⁶ A. Post,¹⁰ J. Powell,³⁸ J. Prasad,¹⁶ V. Predoi,⁹¹ T. Prestegard,⁸⁴ L. R. Price,¹ M. Prijatelj,^{10,36} M. Principe,⁹ S. Privitera,³¹ R. Prix,¹⁰ G. A. Prodi,^{89,90} L. Prokhorov,⁵⁰ O. Puncken,¹⁰ M. Punturo,³⁵ P. Puppó,³⁰ M. Pürerer,³¹ H. Qi,¹⁸ J. Qin,⁵² S. Qiu,¹¹⁵ V. Quetschke,⁸⁸ E. A. Quintero,¹ R. Quitzow-James,⁵⁹ F. J. Raab,³⁹ D. S. Rabeling,²² H. Radkins,³⁹ P. Raffai,⁹³ S. Raja,⁴⁹ C. Rajan,⁴⁹ M. Rakhmanov,⁸⁸ P. Rapagnani,^{80,30} V. Raymond,³¹ M. Razzano,^{20,21} V. Re,²⁷ J. Read,²⁴ C. M. Reed,³⁹ T. Regimbau,⁵⁴ L. Rei,⁴⁸ S. Reid,⁵¹ D. H. Reitze,^{1,6} H. Rew,¹²³ S. D. Reyes,³⁷ F. Ricci,^{80,30} K. Riles,¹⁰¹ M. Rizzo,¹⁰² N. A. Robertson,^{1,38} R. Robie,³⁸ F. Robinet,²⁵ A. Rocchi,¹⁵ L. Rolland,⁸ J. G. Rollins,¹ V. J. Roma,⁵⁹ R. Romano,^{4,5} G. Romanov,¹²³ J. H. Romie,⁷ D. Rosińska,^{132,45} S. Rowan,³⁸ A. Rüdiger,¹⁰ P. Ruggi,³⁶ K. Ryan,³⁹ S. Sachdev,¹ T. Sadecki,³⁹ L. Sadeghian,¹⁸ M. Sakellariadou,¹³³ L. Salconi,³⁶ M. Saleem,¹⁰⁷ F. Salemi,¹⁰ A. Samajdar,¹²⁶ L. Sammut,¹¹⁵ E. J. Sanchez,¹ V. Sandberg,³⁹ B. Sandeen,⁸³ J. R. Sanders,³⁷ B. Sassolas,⁶⁶ P. R. Saulson,³⁷ O. E. S. Sauter,¹⁰¹ R. L. Savage,³⁹ A. Sawadsky,¹⁹ P. Schale,⁵⁹ R. Schilling,^{10,†} J. Schmidt,¹⁰ P. Schmidt,^{1,78} R. Schnabel,²⁹ R. M. S. Schofield,⁵⁹ A. Schönbeck,²⁹ E. Schreiber,¹⁰ D. Schuette,^{10,19} B. F. Schutz,^{91,31} J. Scott,³⁸ S. M. Scott,²² D. Sellers,⁷ A. S. Sengupta,⁹⁶ D. Sentenac,³⁶ V. Sequino,^{27,15} A. Sergeev,¹⁰⁹ Y. Setyawati,^{53,11} D. A. Shaddock,²² T. Shaffer,³⁹ M. S. Shahriar,⁸³ M. Shaltev,¹⁰ B. Shapiro,⁴² P. Shawhan,⁶⁴ A. Sheperd,¹⁸ D. H. Shoemaker,¹² D. M. Shoemaker,⁶⁵

K. Siellez,⁶⁵ X. Siemens,¹⁸ M. Sieniawska,⁴⁵ D. Sigg,³⁹ A. D. Silva,¹³ A. Singer,¹ L. P. Singer,⁶⁹ A. Singh,^{31,10,19} R. Singh,² A. Singhal,¹⁴ A. M. Sintes,¹⁰⁴ B. J. J. Slagmolen,²² J. R. Smith,²⁴ N. D. Smith,¹ R. J. E. Smith,¹ E. J. Son,¹²⁹ B. Sorazu,³⁸ F. Sorrentino,⁴⁸ T. Souradeep,¹⁶ A. K. Srivastava,⁸⁶ A. Staley,⁴¹ M. Steinke,¹⁰ J. Steinlechner,³⁸ S. Steinlechner,³⁸ D. Steinmeyer,^{10,19} B. C. Stephens,¹⁸ R. Stone,⁸⁸ K. A. Strain,³⁸ N. Straniero,⁶⁶ G. Stratta,^{57,58} N. A. Strauss,⁶¹ S. Strigin,⁵⁰ R. Sturani,¹²⁴ A. L. Stuver,⁷ T. Z. Summerscales,¹³⁴ L. Sun,⁸⁵ S. Sunil,⁸⁶ P. J. Sutton,⁹¹ B. L. Swinkels,³⁶ M. J. Szczepańczyk,⁹⁸ M. Tacca,³² D. Talukder,⁵⁹ D. B. Tanner,⁶ M. Tápai,⁹⁷ S. P. Tarabrin,¹⁰ A. Taracchini,³¹ R. Taylor,¹ T. Theeg,¹⁰ M. P. Thirugnanasambandam,¹ E. G. Thomas,⁴⁶ M. Thomas,⁷ P. Thomas,³⁹ K. A. Thorne,⁷ E. Thrane,¹¹⁵ S. Tiwari,^{14,90} V. Tiwari,⁹¹ K. V. Tokmakov,¹⁰⁶ K. Toland,³⁸ C. Tomlinson,⁸⁷ M. Tonelli,^{20,21} Z. Tornasi,³⁸ C. V. Torres,^{88,†} C. I. Torrie,¹ D. Töyrä,⁴⁶ F. Travasso,^{34,35} G. Traylor,⁷ D. Trifirò,²³ M. C. Tringali,^{89,90} L. Trozzo,^{135,21} M. Tse,¹² M. Turconi,⁵⁴ D. Tuyenbayev,⁸⁸ D. Ugolini,¹³⁶ C. S. Unnikrishnan,⁹⁹ A. L. Urban,¹⁸ S. A. Usman,³⁷ H. Vahlbruch,¹⁹ G. Vajente,¹ G. Valdes,⁸⁸ N. van Bakel,¹¹ M. van Beuzekom,¹¹ J. F. J. van den Brand,^{63,11} C. Van Den Broeck,¹¹ D. C. Vander-Hyde,³⁷ L. van der Schaaf,¹¹ J. V. van Heijningen,¹¹ A. A. van Veggel,³⁸ M. Vardaro,^{43,44} S. Vass,¹ M. Vasúth,⁴⁰ R. Vaulin,¹² A. Vecchio,⁴⁶ G. Vedovato,⁴⁴ J. Veitch,⁴⁶ P. J. Veitch,¹¹² K. Venkateswara,¹³⁷ D. Verkindt,⁸ F. Vetrano,^{57,58} A. Viceré,^{57,58} S. Vinciguerra,⁴⁶ D. J. Vine,⁵¹ J.-Y. Vinet,⁵⁴ S. Vitale,¹² T. Vo,³⁷ H. Vocca,^{34,35} C. Vorvick,³⁹ D. V. Voss,⁶ W. D. Voursden,⁴⁶ S. P. Vyatchanin,⁵⁰ A. R. Wade,²² L. E. Wade,¹³⁸ M. Wade,¹³⁸ M. Walker,² L. Wallace,¹ S. Walsh,^{31,10} G. Wang,^{14,58} H. Wang,⁴⁶ M. Wang,⁴⁶ X. Wang,⁷¹ Y. Wang,⁵² R. L. Ward,²² J. Warner,³⁹ M. Was,⁸ B. Weaver,³⁹ L.-W. Wei,⁵⁴ M. Weinert,¹⁰ A. J. Weinstein,¹ R. Weiss,¹² L. Wen,⁵² P. Weßels,¹⁰ T. Westphal,¹⁰ K. Wette,¹⁰ J. T. Whelan,¹⁰² B. F. Whiting,⁶ R. D. Williams,¹ A. R. Williamson,⁹¹ J. L. Willis,¹³⁹ B. Willke,^{19,10} M. H. Wimmer,^{10,19} W. Winkler,¹⁰ C. C. Wipf,¹ H. Wittel,^{10,19} G. Woan,³⁸ J. Woehler,¹⁰ J. Worden,³⁹ J. L. Wright,³⁸ D. S. Wu,¹⁰ G. Wu,⁷ J. Yablon,⁸³ W. Yam,¹² H. Yamamoto,¹ C. C. Yancey,⁶⁴ H. Yu,¹² M. Yvert,⁸ A. Zadrożny,¹¹³ L. Zangrando,⁴⁴ M. Zanolin,⁹⁸ J.-P. Zendri,⁴⁴ M. Zevin,⁸³ L. Zhang,¹ M. Zhang,¹²³ Y. Zhang,¹⁰² C. Zhao,⁵² M. Zhou,⁸³ Z. Zhou,⁸³ S. J. Zhu,^{31,10} X. Zhu,⁵² M. E. Zucker,^{1,12} S. E. Zuraw,¹¹⁹ and J. Zweizig¹

(LIGO Scientific Collaboration and Virgo Collaboration)

¹LIGO, California Institute of Technology, Pasadena, California 91125, USA

²Louisiana State University, Baton Rouge, Louisiana 70803, USA

³American University, Washington, D.C. 20016, USA

⁴Università di Salerno, Fisciano, I-84084 Salerno, Italy

⁵INFN, Sezione di Napoli, Complesso Universitario di Monte S. Angelo, I-80126 Napoli, Italy

⁶University of Florida, Gainesville, Florida 32611, USA

⁷LIGO Livingston Observatory, Livingston, Louisiana 70754, USA

⁸Laboratoire d'Annecy-le-Vieux de Physique des Particules (LAPP), Université Savoie Mont Blanc, CNRS/IN2P3, F-74941 Annecy-le-Vieux, France

⁹University of Sannio at Benevento, I-82100 Benevento, Italy and INFN, Sezione di Napoli, I-80100 Napoli, Italy

¹⁰Albert-Einstein-Institut, Max-Planck-Institut für Gravitationsphysik, D-30167 Hannover, Germany

¹¹Nikhef, Science Park, 1098 XG Amsterdam, The Netherlands

¹²LIGO, Massachusetts Institute of Technology, Cambridge, Massachusetts 02139, USA

¹³Instituto Nacional de Pesquisas Espaciais, 12227-010 São José dos Campos, Sao Paulo, Brazil

¹⁴INFN, Gran Sasso Science Institute, I-67100 L'Aquila, Italy

¹⁵INFN, Sezione di Roma Tor Vergata, I-00133 Roma, Italy

¹⁶Inter-University Centre for Astronomy and Astrophysics, Pune 411007, India

¹⁷International Centre for Theoretical Sciences, Tata Institute of Fundamental Research, Bangalore 560012, India

¹⁸University of Wisconsin-Milwaukee, Milwaukee, Wisconsin 53201, USA

¹⁹Leibniz Universität Hannover, D-30167 Hannover, Germany

²⁰Università di Pisa, I-56127 Pisa, Italy

²¹INFN, Sezione di Pisa, I-56127 Pisa, Italy

²²Australian National University, Canberra, Australian Capital Territory 0200, Australia

²³The University of Mississippi, University, Mississippi 38677, USA

²⁴California State University Fullerton, Fullerton, California 92831, USA

- ²⁵LAL, Univ. Paris-Sud, CNRS/IN2P3, Université Paris-Saclay, F-91898 Orsay, France
- ²⁶Chennai Mathematical Institute, Chennai 603103, India
- ²⁷Università di Roma Tor Vergata, I-00133 Roma, Italy
- ²⁸University of Southampton, Southampton SO17 1BJ, United Kingdom
- ²⁹Universität Hamburg, D-22761 Hamburg, Germany
- ³⁰INFN, Sezione di Roma, I-00185 Roma, Italy
- ³¹Albert-Einstein-Institut, Max-Planck-Institut für Gravitationsphysik, D-14476 Potsdam-Golm, Germany
- ³²APC, AstroParticule et Cosmologie, Université Paris Diderot, CNRS/IN2P3, CEA/Irfu, Observatoire de Paris, Sorbonne Paris Cité, F-75205 Paris Cedex 13, France
- ³³Montana State University, Bozeman, Montana 59717, USA
- ³⁴Università di Perugia, I-06123 Perugia, Italy
- ³⁵INFN, Sezione di Perugia, I-06123 Perugia, Italy
- ³⁶European Gravitational Observatory (EGO), I-56021 Cascina, Pisa, Italy
- ³⁷Syracuse University, Syracuse, New York 13244, USA
- ³⁸SUPA, University of Glasgow, Glasgow G12 8QQ, United Kingdom
- ³⁹LIGO Hanford Observatory, Richland, Washington 99352, USA
- ⁴⁰Wigner RCP, RMKI, H-1121 Budapest, Konkoly Thege Miklós út 29-33, Hungary
- ⁴¹Columbia University, New York, New York 10027, USA
- ⁴²Stanford University, Stanford, California 94305, USA
- ⁴³Università di Padova, Dipartimento di Fisica e Astronomia, I-35131 Padova, Italy
- ⁴⁴INFN, Sezione di Padova, I-35131 Padova, Italy
- ⁴⁵CAMK-PAN, 00-716 Warsaw, Poland
- ⁴⁶University of Birmingham, Birmingham B15 2TT, United Kingdom
- ⁴⁷Università degli Studi di Genova, I-16146 Genova, Italy
- ⁴⁸INFN, Sezione di Genova, I-16146 Genova, Italy
- ⁴⁹RRCAT, Indore Madhya Pradesh 452013, India
- ⁵⁰Faculty of Physics, Lomonosov Moscow State University, Moscow 119991, Russia
- ⁵¹SUPA, University of the West of Scotland, Paisley PA1 2BE, United Kingdom
- ⁵²University of Western Australia, Crawley, Western Australia 6009, Australia
- ⁵³Department of Astrophysics/IMAPP, Radboud University Nijmegen, P.O. Box 9010, 6500 GL Nijmegen, The Netherlands
- ⁵⁴Artemis, Université Côte d'Azur, CNRS, Observatoire Côte d'Azur, CS 34229 Nice cedex 4, France
- ⁵⁵Institut de Physique de Rennes, CNRS, Université de Rennes 1, F-35042 Rennes, France
- ⁵⁶Washington State University, Pullman, Washington 99164, USA
- ⁵⁷Università degli Studi di Urbino "Carlo Bo," I-61029 Urbino, Italy
- ⁵⁸INFN, Sezione di Firenze, I-50019 Sesto Fiorentino, Firenze, Italy
- ⁵⁹University of Oregon, Eugene, Oregon 97403, USA
- ⁶⁰Laboratoire Kastler Brossel, UPMC-Sorbonne Universités, CNRS, ENS-PSL Research University, Collège de France, F-75005 Paris, France
- ⁶¹Carleton College, Northfield, Minnesota 55057, USA
- ⁶²Astronomical Observatory Warsaw University, 00-478 Warsaw, Poland
- ⁶³VU University Amsterdam, 1081 HV Amsterdam, The Netherlands
- ⁶⁴University of Maryland, College Park, Maryland 20742, USA
- ⁶⁵Center for Relativistic Astrophysics and School of Physics, Georgia Institute of Technology, Atlanta, Georgia 30332, USA
- ⁶⁶Laboratoire des Matériaux Avancés (LMA), CNRS/IN2P3, F-69622 Villeurbanne, France
- ⁶⁷Université Claude Bernard Lyon 1, F-69622 Villeurbanne, France
- ⁶⁸Università di Napoli "Federico II," Complesso Universitario di Monte S. Angelo, I-80126 Napoli, Italy
- ⁶⁹NASA/Goddard Space Flight Center, Greenbelt, Maryland 20771, USA
- ⁷⁰RESCEU, University of Tokyo, Tokyo 113-0033, Japan
- ⁷¹Tsinghua University, Beijing 100084, China
- ⁷²Texas Tech University, Lubbock, Texas 79409, USA
- ⁷³Pennsylvania State University, University Park, Pennsylvania 16802, USA
- ⁷⁴National Tsing Hua University, Hsinchu City, 30013 Taiwan, Republic of China
- ⁷⁵Charles Sturt University, Wagga Wagga, New South Wales 2678, Australia
- ⁷⁶West Virginia University, Morgantown, West Virginia 26506, USA
- ⁷⁷University of Chicago, Chicago, Illinois 60637, USA
- ⁷⁸Caltech CaRT, Pasadena, California 91125, USA

- ⁷⁹*Korea Institute of Science and Technology Information, Daejeon 305-806, Korea*
- ⁸⁰*Università di Roma “La Sapienza,” I-00185 Roma, Italy*
- ⁸¹*University of Brussels, Brussels 1050 Belgium*
- ⁸²*Sonoma State University, Rohnert Park, California 94928, USA*
- ⁸³*Center for Interdisciplinary Exploration and Research in Astrophysics (CIERA), Northwestern University, Evanston, Illinois 60208, USA*
- ⁸⁴*University of Minnesota, Minneapolis, Minnesota 55455, USA*
- ⁸⁵*The University of Melbourne, Parkville, Victoria 3010, Australia*
- ⁸⁶*Institute for Plasma Research, Bhat, Gandhinagar 382428, India*
- ⁸⁷*The University of Sheffield, Sheffield S10 2TN, United Kingdom*
- ⁸⁸*The University of Texas Rio Grande Valley, Brownsville, Texas 78520, USA*
- ⁸⁹*Università di Trento, Dipartimento di Fisica, I-38123 Povo, Trento, Italy*
- ⁹⁰*INFN, Trento Institute for Fundamental Physics and Applications, I-38123 Povo, Trento, Italy*
- ⁹¹*Cardiff University, Cardiff CF24 3AA, United Kingdom*
- ⁹²*Montclair State University, Montclair, New Jersey 07043, USA*
- ⁹³*MTA Eötvös University, “Lendulet” Astrophysics Research Group, Budapest 1117, Hungary*
- ⁹⁴*National Astronomical Observatory of Japan, 2-21-1 Osawa, Mitaka, Tokyo 181-8588, Japan*
- ⁹⁵*School of Mathematics, University of Edinburgh, Edinburgh EH9 3FD, United Kingdom*
- ⁹⁶*Indian Institute of Technology, Gandhinagar Ahmedabad Gujarat 382424, India*
- ⁹⁷*University of Szeged, Dóm tér 9, Szeged 6720, Hungary*
- ⁹⁸*Embry-Riddle Aeronautical University, Prescott, Arizona 86301, USA*
- ⁹⁹*Tata Institute of Fundamental Research, Mumbai 400005, India*
- ¹⁰⁰*INAF, Osservatorio Astronomico di Capodimonte, I-80131 Napoli, Italy*
- ¹⁰¹*University of Michigan, Ann Arbor, Michigan 48109, USA*
- ¹⁰²*Rochester Institute of Technology, Rochester, New York 14623, USA*
- ¹⁰³*NCSA, University of Illinois at Urbana-Champaign, Urbana, Illinois 61801, USA*
- ¹⁰⁴*Universitat de les Illes Balears, IAC3—IEEC, E-07122 Palma de Mallorca, Spain*
- ¹⁰⁵*University of Białystok, 15-424 Białystok, Poland*
- ¹⁰⁶*SUPA, University of Strathclyde, Glasgow G1 1XQ, United Kingdom*
- ¹⁰⁷*IISER-TVM, CET Campus, Trivandrum Kerala 695016, India*
- ¹⁰⁸*Canadian Institute for Theoretical Astrophysics, University of Toronto, Toronto, Ontario M5S 3H8, Canada*
- ¹⁰⁹*Institute of Applied Physics, Nizhny Novgorod 603950, Russia*
- ¹¹⁰*Pusan National University, Busan 609-735, Korea*
- ¹¹¹*Hanyang University, Seoul 133-791, Korea*
- ¹¹²*University of Adelaide, Adelaide, South Australia 5005, Australia*
- ¹¹³*NCBJ, 05-400 Świerk-Otwock, Poland*
- ¹¹⁴*IM-PAN, 00-956 Warsaw, Poland*
- ¹¹⁵*Monash University, Victoria 3800, Australia*
- ¹¹⁶*Seoul National University, Seoul 151-742, Korea*
- ¹¹⁷*The Chinese University of Hong Kong, Shatin, New Territories, Hong Kong SAR, China*
- ¹¹⁸*University of Alabama in Huntsville, Huntsville, Alabama 35899, USA*
- ¹¹⁹*University of Massachusetts-Amherst, Amherst, Massachusetts 01003, USA*
- ¹²⁰*ESPCI, CNRS, F-75005 Paris, France*
- ¹²¹*Università di Camerino, Dipartimento di Fisica, I-62032 Camerino, Italy*
- ¹²²*Southern University and A&M College, Baton Rouge, Louisiana 70813, USA*
- ¹²³*College of William and Mary, Williamsburg, Virginia 23187, USA*
- ¹²⁴*Instituto de Física Teórica, University Estadual Paulista/ICTP South American Institute for Fundamental Research, São Paulo São Paulo 01140-070, Brazil*
- ¹²⁵*University of Cambridge, Cambridge CB2 1TN, United Kingdom*
- ¹²⁶*IISER-Kolkata, Mohanpur, West Bengal 741252, India*
- ¹²⁷*Rutherford Appleton Laboratory, HSIC, Chilton, Didcot, Oxon OX11 0QX, United Kingdom*
- ¹²⁸*Whitman College, 345 Boyer Avenue, Walla Walla, Washington 99362 USA*
- ¹²⁹*National Institute for Mathematical Sciences, Daejeon 305-390, Korea*
- ¹³⁰*Université de Lyon, F-69361 Lyon, France*
- ¹³¹*Hobart and William Smith Colleges, Geneva, New York 14456, USA*
- ¹³²*Janusz Gil Institute of Astronomy, University of Zielona Góra, 65-265 Zielona Góra, Poland*
- ¹³³*King’s College London, University of London, London WC2R 2LS, United Kingdom*
- ¹³⁴*Andrews University, Berrien Springs, Michigan 49104, USA*
- ¹³⁵*Università di Siena, I-53100 Siena, Italy*

¹³⁶*Trinity University, San Antonio, Texas 78212, USA*

¹³⁷*University of Washington, Seattle, Washington 98195, USA*

¹³⁸*Kenyon College, Gambier, Ohio 43022, USA*

¹³⁹*Abilene Christian University, Abilene, Texas 79699, USA*

[†]Deceased.